TR-104

TECHNICAL REPORT

ASWEPS REPORT NO. 5

PREDICTION OF THE THERMOCLINE DEPTH

P. A. MAZEIKA

Formulation Branch
Oceanographic Prediction Division

JUNE 1960

U. S. NAVY HYDROGRAPHIC OFFICE
WASHINGTON 25, D. C.
Price $1.05

ABSTRACT

In order to derive a method of predicting thermocline depth, BT data and associated weather conditions at the Atlantic Ocean Weather Station (OWS) CHARLIE (52°N, 35°W) were studied. Selected groups of bathythermograms covering one or several days were used to compute mean level of the interface between the mixed layer and the thermocline. Velocity and vertical extent of pure wind current are considered to be proportional to the surface wind-wave parameters. A mixing parameter, k, which is a function of wave amplitude A, wave length λ, and mixed-layer thickness h, has been determined from the BT groups and associated weather data. Mixing parameter k is considered to be proportional to the vertical component of the mixing length at the interface of the mixed layer and the thermocline. As a function of sea state parameter η and stability index Δt, mixing parameter k is applied to mean thermocline depth prediction by use of different functional curves for sea state in uniform current flow or in convergent and divergent current conditions.

FOREWORD

The Hydrographic Office has been assigned the responsibility for the development of an Antisubmarine Warfare Environmental Prediction System (ASWEPS). This system is designed to provide the Fleet with continuing environmental information and predictions in support of anti-submarine warfare operations.

Development of analytical methods of prediction plays an important part in the research portion of this program.

This report describes a method of predicting the depth of the thermocline or layer of rapid temperature and salinity changes in the oceans from consideration of wind stress and certain other meteorological and oceanographic conditions. It embodies the results of research conducted by the author with the cooperation of the United States Coast Guard.

It is believed that this report will contribute to the understanding of the physical processes in the oceans and will aid in the development of a generalized technique for prediction of the thermal structure of the oceans.

E. C. STEPHAN
Rear Admiral, U. S. Navy
Hydrographer

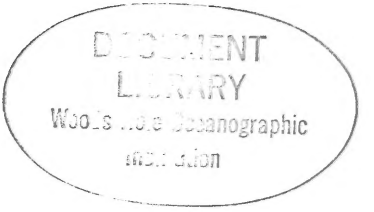

CONTENTS

INTRODUCTION

Notes on Data

Bathythermograms (BT's), weather charts, and simultaneous weather and wave observations were used to determine the functional relationship between parameters of mixing, stability, convergence or divergence, and wind waves. For this purpose, a large amount of continuous data was required from the same observation point over several years. Only an extreme minimum of this requirement was satisfied. BT's taken by various Atlantic Ocean weather ships and processed (corrected, printed on cards, and catalogued) by the BT Branch, National Oceanographic Data Center, were available for the years 1949 through 1954. Data of Ocean Weather Station (OWS) CHARLIE (52°48' N, 35°30' W) were selected for the basic computations, because this station offered a fair amount of data and appeared to be affected less than other weather stations by permanent and semi-permanent currents. However, not all of the approximately 5,000 BT's of station CHARLIE were applicable; sporadic BT's could not be used. Many BT casts did not reach the thermocline; glass BT slides often are either scratched and rendered illegible or may show unexplainable inconsistencies of temperature and depth when compared with observations taken a few hours earlier or later. After all deficient BT's were discarded, the remainder was about 30 percent of the total.

BT's from weather stations and other ships were mainly taken under fair weather conditions; rough weather BT's are scarce. The latter circumstance makes extraction of consistent information on upper layer properties and their variations more difficult.

Data from weather stations BRAVO (56°30' N, 51° W), ECHO (35° N, 48° W), and DELTA (44° N, 41° W) were used for testing the prediction method. Two tests were made at each of these stations using BT's from 1949 through 1954. Each test consisted of about 30 observations selected at random from the 6-year period. Each observation was a group with more than three BT's taken over a period of at least 24 hours.

BT's of station CHARLIE were processed for 1956 and 1957; however, they were not included in the computations of the mixing factor. Therefore, two tests were also conducted using the data from this station.

The Bathythermogram

Although general concepts and names exist for various layers and boundaries indicated by a BT, various observers often interpret the mixed-layer depth, vertical extent of the thermocline, and other characteristics of the upper layers differently. Some BT's do not show definite or distinct boundaries; furthermore, no generally accepted criteria exist for their interpretation. Figure 1 shows some typical BT traces with their parts and various elements defined as used in this study.

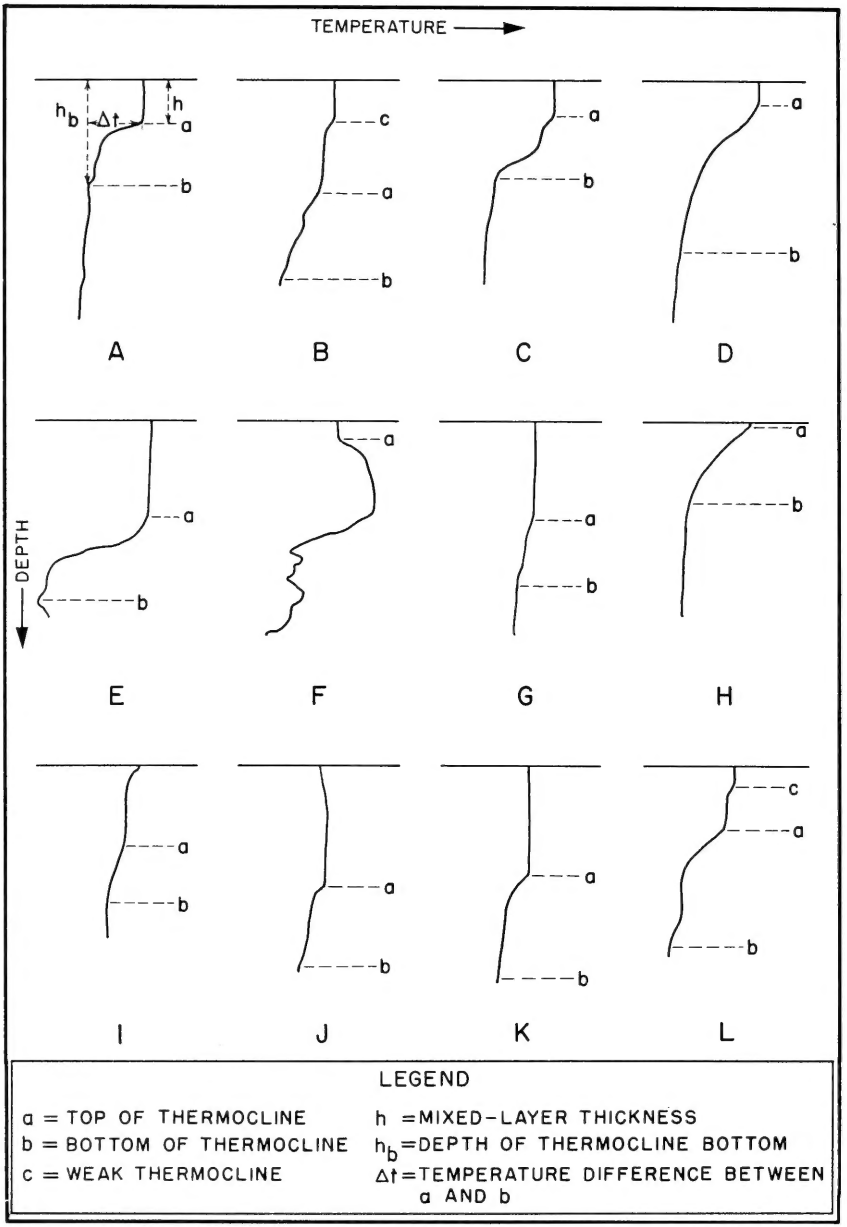

FIGURE I TYPICAL BT TRACES

Figure 1-A is the simplest type; levels a and b are easily located; and the sharp turn (almost 90°) of the trace at the interface indicates active mixing and probable horizontal flow in different directions in the mixed layer and the thermocline. The various levels are less certain in Figures 1-C and 1-J, the traces in Figures 1-G and 1-I curve mildly, and Figures 1-C and 1-I indicate a decaying mixed layer. Level c in Figures 1-B and 1-L show weak thermoclines. A weak thermocline is a small thermocline within the mixed layer.

The depth of the thermocline bottom is not always easily determined; there may be considerable difference in evaluation. Sometimes a decisive change in temperature gradient occurs as seen in Figures 1-A and 1-C. Normally, the gradient is very weak and decreases slowly as seen in Figures 1-B, 1-D, 1-H, 1-K, and 1-L. In these particular cases, the thermocline bottom is established as a level where the temperature gradient is less than 1° F per 50 feet. The exact depth is irrelevant, because variation of temperature below the thermocline is slight. Evaluation of Δt (temperature difference between the sea surface and the bottom of the thermocline) will vary little, even if evaluation of the depth of the thermocline bottom varies considerably. The temperature at a given depth below which the thermocline bottom migrates only in winter would be the best reference level for determination of Δt. For existing BT data, the 400-foot depth is most convenient, because traces often end shortly after reaching this depth.

When there is a positive gradient in the thermocline (Figure 1-F), stability of the thermocline is uncertain; the water mass comprising the mixed layer will often become unstable and sink; and a deep mixed layer will be produced by the instability mixing process. Sometimes water masses with a positive gradient are stable, because considerably higher salinity water in the thermocline balances the cold, less saline water in the mixed layer.

Figures 1-I and 1-J show surface effects of warming and cooling, respectively. Figure 1-H indicates the origination of or the vanishing of a mixed layer.

Reliability of the Bathythermograph

Bathythermographs are not precise instruments, and they often lose calibration. Comparison of a bathythermogram and plotted temperatures of a Nansen cast taken simultaneously yields satisfactory agreement most of the time. The greatest discrepancies of temperature and depth usually occur in the thermocline.

BT temperature corrections based on the average difference between bucket or injection temperatures and the surface temperature of the BT are made during processing. The mean error probably does not exceed 1° F. Actual temperature values are irrelevant in this prediction method; temperature differences between various depths in a BT are of more interest. Comparisons with simultaneous Nansen casts provide evidence that temperature differences are more reliable than actual temperatures.

Temperature differences and their variations with depth from 26 Nansen casts and BT's taken simultaneously in the upper layers in September 1960 at station CHARLIE are listed in Table 1. The range of surface temperature differences between the Nansen casts and BT's was 2.1° F (0.2° to 2.3°); the range of differences below the thermocline was 2.35° F (0.15° to 2.50°); and the range of variation between the surface difference and the difference below the thermocline was 0.9° F (from 0° to 0.9°).

TABLE 1

TEMPERATURE DIFFERENCES AND VARIATIONS BETWEEN SIMULTANEOUS NANSEN AND BT CASTS AT THE SURFACE AND BELOW THE THERMOCLINE

SURFACE		BELOW THERMOCLINE		RANGE	
Temperature difference (°F)	Percent	Temperature difference (°F)	Percent	Variation (°F)	Percent
0-0.5	15	0-0.5	15	0	27
≥0.5	85	≥0.5	85	0-0.5	62
≥1.0	38	≥1.0	50	0.5-0.9	11
≥1.5	27	≥1.5	35		
≥2.0	15	≥2.0	15		

Seven different bathythermographs were used in this series of 26 observations. The results may be considered fairly representative of most of the BT data. The error of temperature differences measured between the sea surface and any depth in the lower part of the thermocline or below the thermocline is generally smaller than 0.5° F.

Depth can be read on a 450-foot BT trace with accuracy of approximately 5 feet, yet little is known about the reliability of the existing BT data with respect to depth. There are no references similar to bucket and injection temperatures for checking depth.

There is a case in the Hydrographic Office data where the USS SAN PABLO and USS REHOBOTH operated only a few miles from each other. The 34 BT's taken on the REHOBOTH during one day placed the mean layer depth at 157 feet with an oscillation of 25 feet about the mean. Approximately the same number of BT's taken by the SAN PABLO during the same time interval, however, shows the mean layer depth at 128 feet with about the same degree of oscillation. This indicates a difference in mean layer depth of 29 feet. Apparently one bathythermograph had lost calibration.

There is no way of determining the number of similarly inconsistent BT's in the existing data. Some evidence could be collected to compare the mean thermocline depth computed from the last 5 or 6 BT's of a station

with the mean thermocline depth computed from a similar number of the first BT's taken by a relief ship. The BT observations must be made by both ships in a 2- to 3-day period, when the weather and other conditions remain constant for several days before and after relief. Not many cases satisfy these requirements; examination of 7 years of data from station ECHO for the months of July, August, and September reveals only six cases satisfactory for comparison. The mean thermocline depths ($\bar{h}$) were computed for departing and relief ships, and the mean difference ($\overline{\Delta h}$) of these six observations was 6.8 feet. The degree of accuracy seems to be of the same order as the approximation of depths on a bathythermogram. Severe inconsistencies, as given in the example above (SAN PABLO and REHOBOTH), are probably not too numerous.

A more serious drawback is irregularity and non-continuity of BT observations. In addition, BT's are not always taken at the same location; positions may vary constantly within approximately a 30-mile radius. It is difficult to apply such observations to a detailed study of internal waves or other similar problems, even though they were taken regularly and at sufficiently short intervals of time.

Mean Level

The interface between the mixed layer and the thermocline constantly oscillates vertically owing to internal waves. The mean level about which this oscillation occurs can be compared to the mean level of surface waves.

One BT observation gives an instantaneous thermocline depth, $h = \bar{h}+z$, where $\bar{h}$ is the mean thermocline depth (Figure 2), and z is the elevation or depression with respect to $\bar{h}$ at the instant of observation. The mean periods of internal wave spectra are longer than the mean periods of surface wind-wave spectra; therefore, a group of BT's covering a period of at least 24 hours is required for computation of the mean thermocline depth. A group of BT's is considered satisfactory: (1) if the thermocline is in a steady state, that is, not in the process of changing during the period covered by the group; (2) when complete weather data and weather charts are available for a period of at least 15 days preceding the BT group; and (3) if the BT's in the group occur at regular intervals of time.

About 356 groups in the BT data of station CHARLIE approximated or satisfied these requirements at the time of this study. Some of these groups consisted of more than 30 BT's covering periods of several days; some were limited to 3 BT's in one day.

Internal Waves

A systematic study of internal waves was not attempted after analysis of the selected BT groups, because of deficiencies previously indicated in the data. However, the range of oscillation about the mean level of the interface was recorded for all groups of more than 3 BT's. These oscillation ranges are assumed to represent the approximate amplitudes of internal

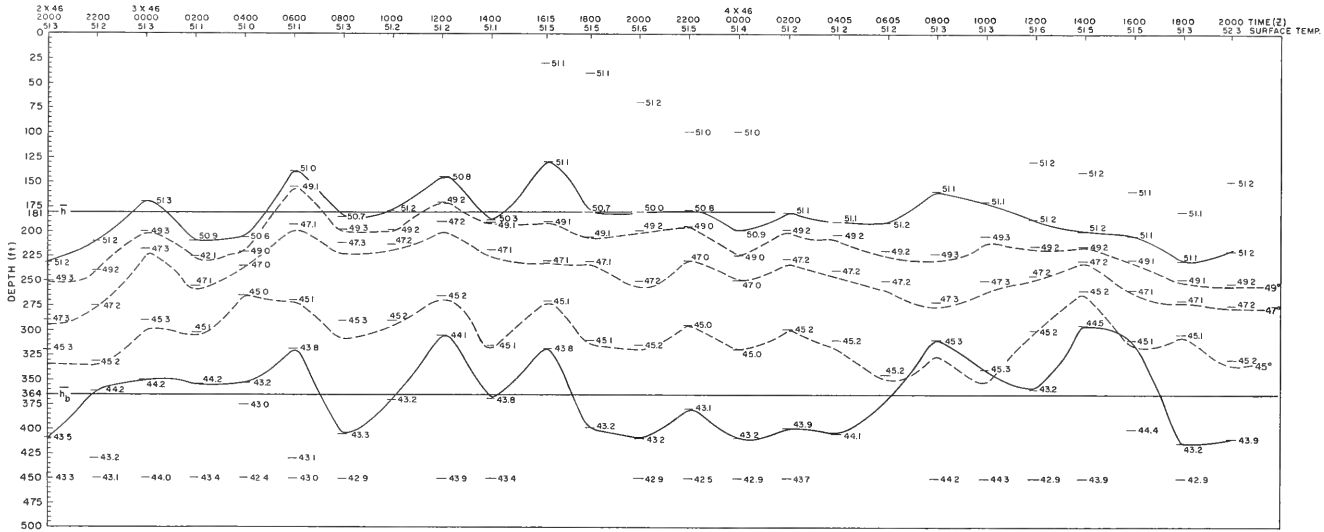

FIGURE 2 INTERNAL WAVES AT THE TOP AND BOTTOM OF THE THERMOCLINE

waves at the interface between the mixed layer and the thermocline. The frequency distribution, mean, and standard deviation were computed for the oscillation ranges of 300 groups. The results are shown in Figure 3.

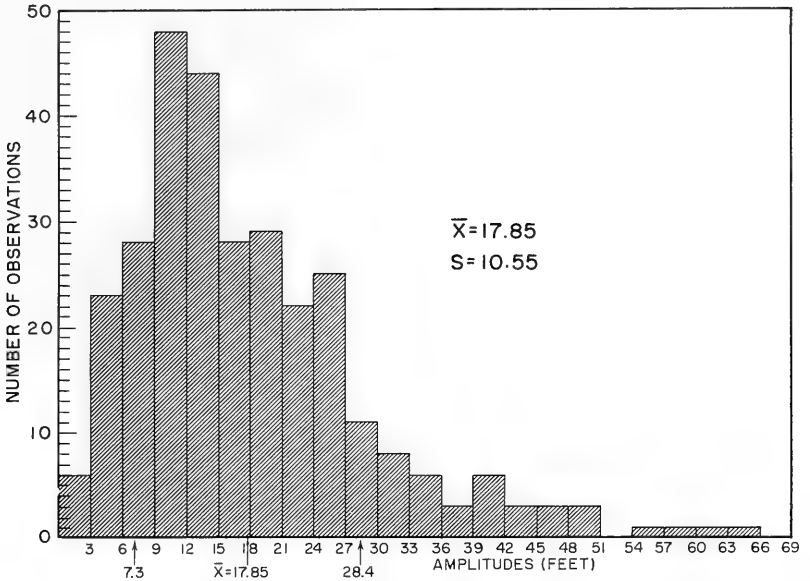

FIGURE 3 AMPLITUDES OF INTERNAL WAVES: FREQUENCY DISTRIBUTION, MEAN, AND STANDARD DEVIATION. (OBS. 300)

The vertical axis represents the number of observations; the horizontal axis represents 3-foot amplitude classes. The mean value is 17.85 feet, the standard deviation is 10.55 feet, and the highest frequency occurs in the 9- to 12-foot class. Large amplitudes of internal waves were usually found to be associated with the slow passage of strong weather disturbances causing divergent or convergent flow in the upper layers.

Divergence is produced in the center of a cyclonic low or along a well-defined front where winds with large fetches on both sides of the front change direction quite sharply in the frontal zone. The thermocline becomes considerably shallower in the frontal area, and the internal wave propagates with the front. The front may disintegrate or begin to move away rapidly, leaving the original internal wave lagging behind. In either case the divergent wave will probably become a standing wave which will continue to oscillate in the area for several days and become superimposed on the internal-wave spectrum of tidal and shorter periods.

Recurring divergence or convergence increases the duration and range of large oscillations. The thermocline depth oscillated between 90 and 170 feet on 22 and 23 September 1954 in the area of station CHARLIE. These large amplitudes of internal waves were probably caused by slowly propagating fronts and wind fields passing in succession during these and previous days (Figure 4).

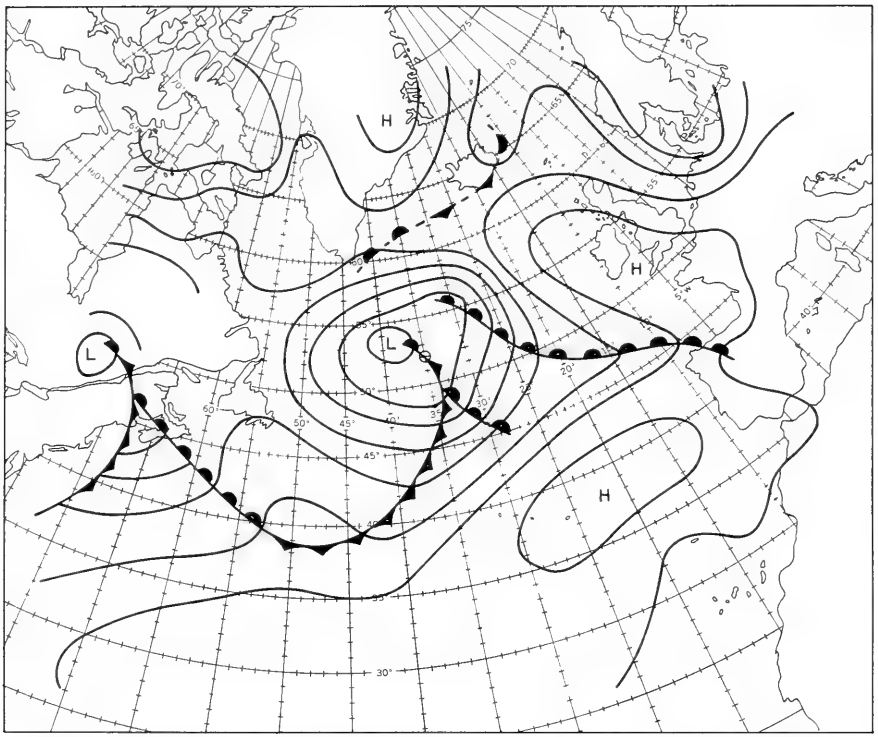

FIGURE 4 POSITIONS OF FRONTS WITH RESPECT TO THE OBSERVATION POINT (52° 48' N, 35° 30' W) — 1230Z, 22 SEPTEMBER 1954

Internal waves with long periods and moderate amplitudes are shown in Figure 2. The temperature values, plotted every 2 hours for 2 days, were taken from BT's of station CHARLIE. The upper solid line in the figure represents the interface between the mixed layer and the thermocline; the lower solid line is the bottom of the thermocline; and the broken lines are isotherms of 45°, 47°, and 49° F. Numbers within the figure indicate solitary temperature values at various levels.

The period of the waves at the top and bottom of the thermocline is about 6 hours; however, the amplitude of oscillation is usually larger at the bottom. Both wave systems appear to be quite independent: they may or may not be in phase. The temperature gradient in the thermocline is not constant but varies continually, sometimes slowly, sometimes rapidly, according to the phase or amplitude relationship of the internal-wave systems at the top and bottom of the thermocline.

Large amplitude internal waves at the bottom of the thermocline are shown in Figure 5. The interface between the mixed layer and the thermocline is shown by the solid line. Temperature values in the interface

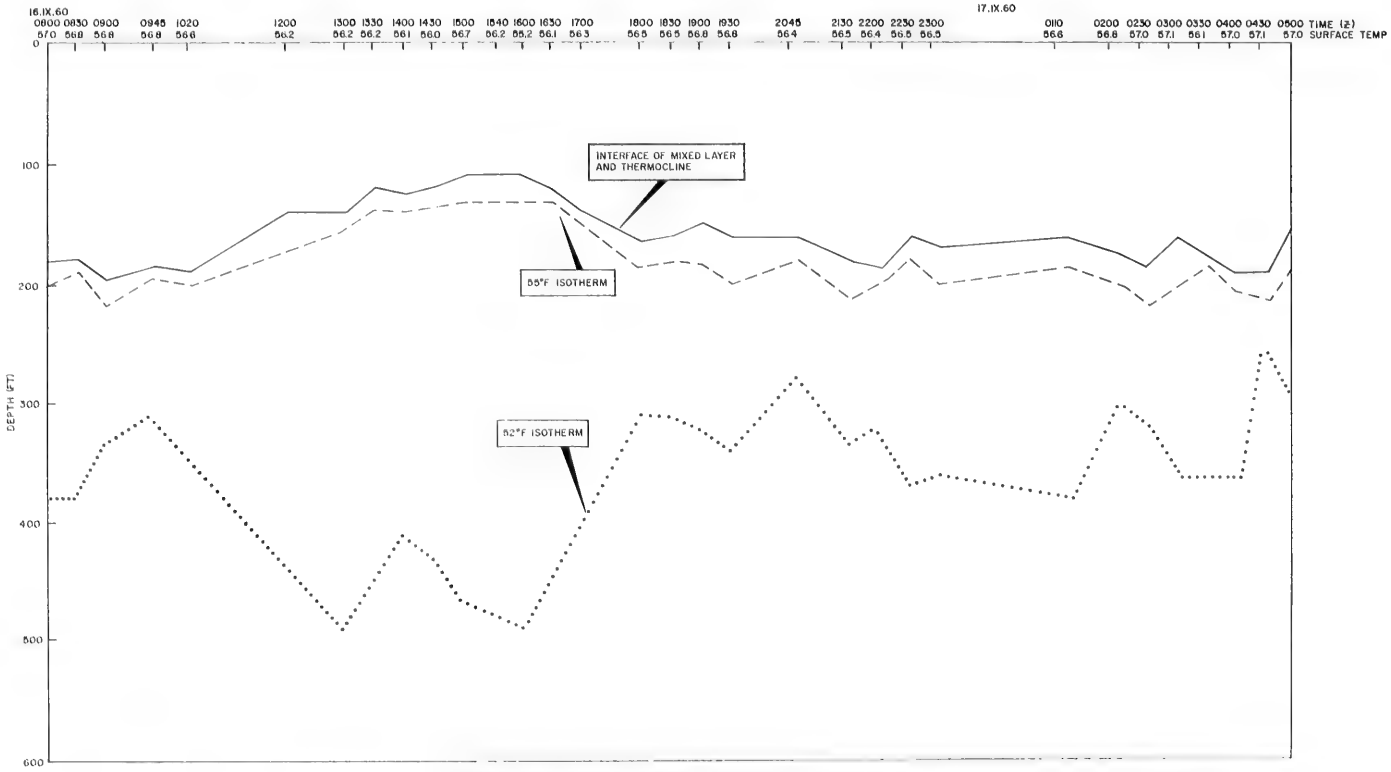

FIGURE 5 VARIATION OF TEMPERATURE DISTRIBUTION DUE TO INTERNAL WAVES AT THE TOP AND THE BOTTOM OF THE THERMOCLINE

are approximately equal to the surface temperatures shown along the upper margin of the figure. For purposes of further outlining the internal-wave forms, the 55-degree isotherm (broken line) in the upper part of the thermocline and the 52-degree isotherm (dotted line) in the lower part of the thermocline were plotted. The BT's used in this figure were taken from a drifting ship approximately 100 nautical miles south of OWS CHARLIE.

Short-period internal waves at the top and bottom of the thermocline are shown in Figure 6 which is constructed from BT's taken every 3 to 4 minutes. Temperature values are given at the surface and 350-foot depth. Periods of the internal waves range from about 5 to 9 minutes; amplitudes are about 5 feet. These short-period waves are superimposed on tidal and longer period internal waves.

Strong eddies produced by tidal currents meeting at right angles may considerably reduce or even destroy surface waves. Heavy rain may also reduce surface waves. This reduction is apparently due to turbulence created in a limited surface layer. In like manner, turbulence at the interface of the mixed layer and thermocline may also be expected to hamper internal waves. Evidence in direct support of this assumption is not available; however, there is a general impression that active mechanical mixing diminishes the oscillations of the interface during periods of increasing thermocline depth.

THEORY

Mixing

Mass exchange between the sea surface and the top of the thermocline forms the mixed layer. Water particles must move vertically through the entire mixed layer, either in one continuous motion or by intermittent steps from one level to another. The latter is more likely to occur in all types of mixing.

The main types of mixing considered decisive in the formation of the mixed layer are: (1) instability mixing produced by sinking of dense water; (2) mixing due to rising or sinking of water caused by divergence or convergence; and (3) mechanical mixing, a turbulent transfer of momentum from one level to another by combined action of wind waves and associated wind currents. All three types of mixing often occur simultaneously, especially in autumn, when mixing action is more effective, that is, faster and deeper.

Instability Mixing Due to Advection

In areas where vertical boundaries exist, tongue-like advections of warm water beneath cold water masses or cold water flowing over warm water create unstable situations. If the density of the overlying cold water is greater, instability mixing takes place quite rapidly either with or without the help of mechanical mixing. Such situations occur frequently at station DELTA. An example is shown in Figure 7. The cold mixed layer

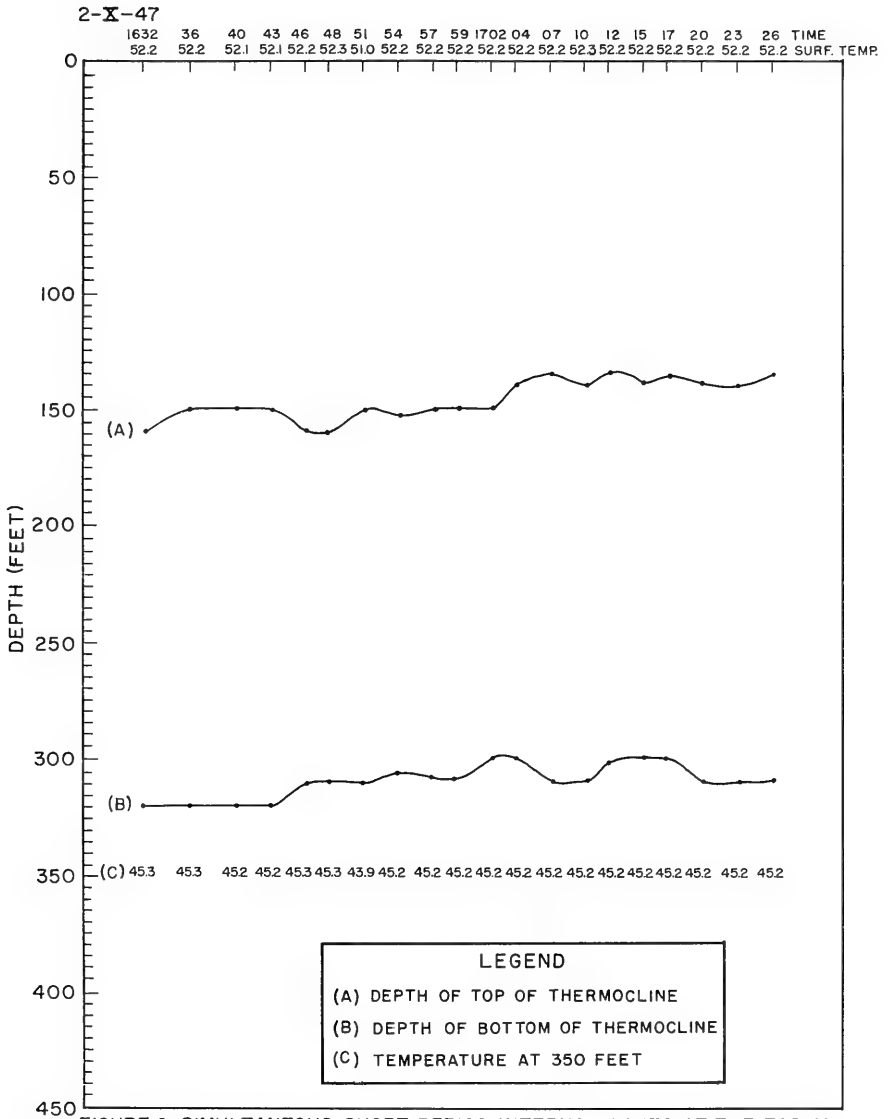

FIGURE 6 SIMULTANEOUS SHORT-PERIOD INTERNAL WAVES AT THE TOP AND BOTTOM OF THE THERMOCLINE

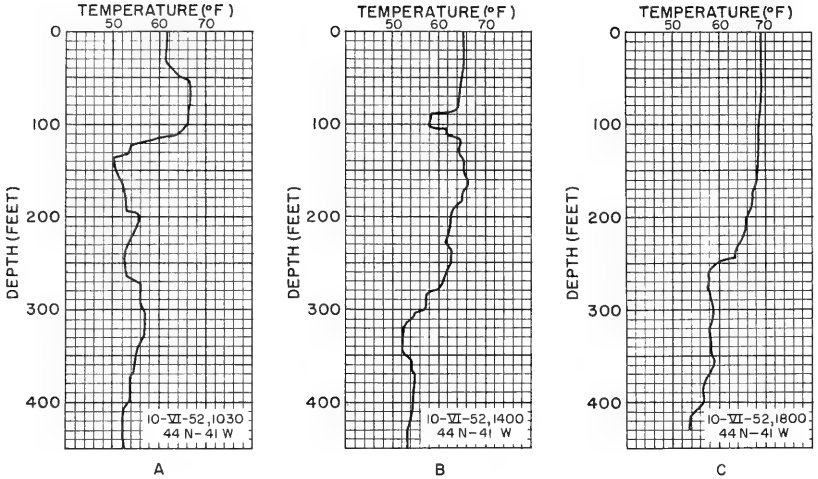

FIGURE 7 INSTABILITY MIXING DUE TO ADVECTION

overlies a warm water intrusion at depths between 30 and 110 feet (Figure 7A). Three and one-half hours later (Figure 7B) the mixed layer increased 55 feet in thickness. Winds of Beaufort force 4 to 5 and sea state 4 could perform slower mixing to approximately the same depth. During the period of mixing more warm water intruded at depths between 110 and 300 feet, while a tongue of cold water intruded between 300 and 420 feet (Figure 7B). Figure 7C shows the effect of 6 additional hours of instability mixing; the mixed-layer depth has increased to 160 feet.

Prediction of thermocline depths could be made under these conditions only when the motion and properties of the water masses are known. Detailed observations for several days in the prediction area would be necessary to permit a prediction to be made only a few days in advance.

Instability Mixing Due to Density Increase

Evaporation and/or cooling increase the density of surface water. These are further sources of instability mixing, especially in autumn and winter. If evaporation or cooling or both increase the density of surface water during a certain period of time, the denser water sinks to a level of equivalent density. The extent of sinking in the thermocline depends on the vertical density gradient $G = \frac{\partial \rho}{\partial z}$. A sharp gradient limits the sinking distance; a slight gradient permits considerable sinking. Less dense water from the mixed layer and from the upper part of the thermocline replaces the sinking water. The mechanism of density transformation occurs within a thin surface stratum; density does not increase sharply, because mixing is continuous.

If no mixing process other than instability mixing occurs during a given time interval, the increase (Δh) of the mixed-layer thickness is

(1) inversely proportional to the previous mixed-layer thickness (h), (2) inversely proportional to the mean density gradient ($\bar{G}$) in the thermocline, and (3) directly proportional to the amount of denser water ($M = \int \frac{dM}{dt} dt$) produced at the surface during the given time period. An expression combining these factors is:

$$\Delta h = \frac{R}{h\bar{G}} \int \frac{dM}{dt} dt \qquad (1)$$

where R is a proportionality factor dependent on type of units used, amount of water added from the thermocline, horizontal components of motion associated with the increase of density, conduction of heat from and to the mixed layer below the thin surface stratum of density change, and local conditions such as permanent flow, convergence or divergence, etc. Thus the proportionality factor is a sum of several minor or individually nondeterminable components and can hardly be expected to remain constant; however, it can probably be treated as a constant in practical use for at least more or less restricted areas. If sufficiently accurate determinations of the increase of mixed-layer density and of mean density gradient in the thermocline could be made in a case where only instability mixing occurs, the factor R could be determined empirically.

During spring the increasing temperature gradient in the thermocline constantly increases stability. If no advection occurs, small variations of salinity caused by evaporation cannot offset this increasing stability; hence, instability mixing can be neglected. Instability mixing is also negligible during summer because of limited evaporation, increasing surface temperature, and the magnitude of the density gradient in the thermocline.

Instability mixing becomes important during late fall, when surface cooling starts to reduce the temperature gradient in the thermocline. At this same time, wind waves and drift caused by severe storms increase the mixed-layer thickness to nearly the maximum possible by mechanical mixing. Rapid cooling and active evaporation, which cause instability mixing, usually occur with heavy seas.

Subsequent to a fall storm, a thermocline deeper than one produced by mechanical mixing can be expected. Under given stability and surface conditions, the thermocline depth is determined by the combined effects of mechanical mixing and instability mixing. If a storm with slightly deeper mixing penetration occurs soon after another storm, the thermocline depth, which is already beyond the influence of mechanical mixing, would not be altered. As surface cooling proceeds, further mixing and increase of the thermocline depth are caused only by instability mixing. The influence of mechanical mixing on the thermocline depth gradually ceases. Even the heaviest storms during winter do not affect the thermocline, because turbulence does not extend to the bottom of the mixed layer.

Mixing Due to Permanent Convergence or Divergence

In areas of permanent or semipermanent convergence or divergence, water particles have vertical components of motion, thus fulfilling conditions of mass interchange between the surface and bottom of the mixed layer. The processes involved in this type of mixing are not explicit. A possible explanation is that downward motion of water in a convergence zone creates turbulence at the top of the thermocline, and increases the mixed-layer thickness to a certain extent. However, the downward motion does not penetrate to the bottom of the thermocline; and, after the mixed-layer thickness reaches a steady state, further circulation takes place only within the layer.

In case of divergence, upward movement of water causes denser thermocline water to rise, resulting in reduction of the thickness. After a balance is reached between the rate of divergence and reduction of the mixed-layer thickness, further circulation is again limited to the layer and does not cross the interface between the mixed layer and the thermocline.

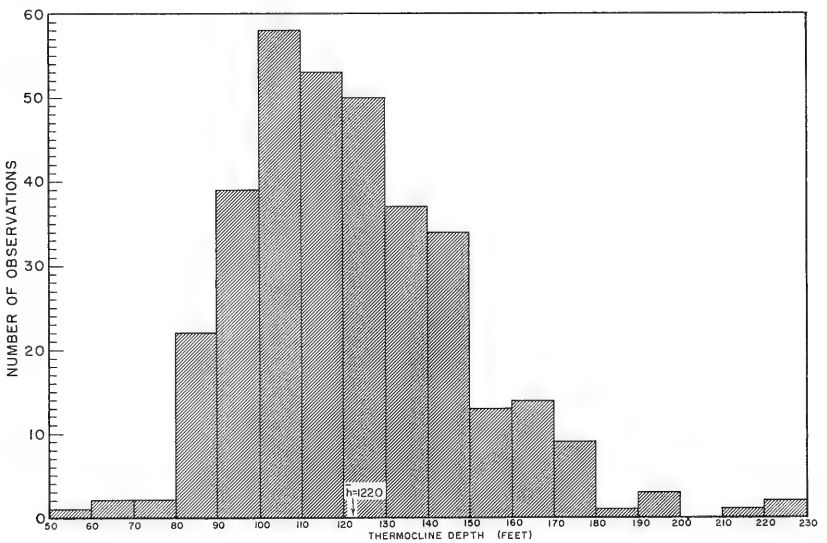

FIGURE 8 FREQUENCY DISTRIBUTION OF THERMOCLINE DEPTHS AT OCEAN WEATHER STATION ECHO (35° N, 48° W) IN SEPTEMBER (6 YEARS' DATA, 1949–1954, 341 OBS)

OWS ECHO appears to lie in a semipermanent convergence area during late summer and autumn. Figure 8 shows the frequency distribution of thermocline depths computed from 6 years of data at OWS ECHO for September. The thermocline was between 80 and 150 feet 86 percent of the time, whereas it was between 50 and 80 feet only 1.5 percent of the time. There were no observed thermocline depths of less than 50 feet; 12.5 percent were between

150 and 230 feet. The mean thermocline depth is quite constant during individual years. Dispersion over the range between 80 and 150 feet is attributed to variability of convergence from year to year. Thermocline depths exceeding 150 feet are probably caused by very strong convergence produced by hurricanes passing between OWS ECHO and the east coast of the United States.

Figure 9 shows the frequency distribution of wind force at OWS ECHO for September for the same 6 years. Wind force was Beaufort 3 or less 58 percent of the time. Under existing stability conditions the corresponding thermocline depth should be no more than 10 feet. Wind force was Beaufort 4 and 5, 34 percent of the time, corresponding to a thermocline depth of about 70 feet. The wind was strong enough to cause thermocline depths between 70 and 110 feet only 8 percent of the time.

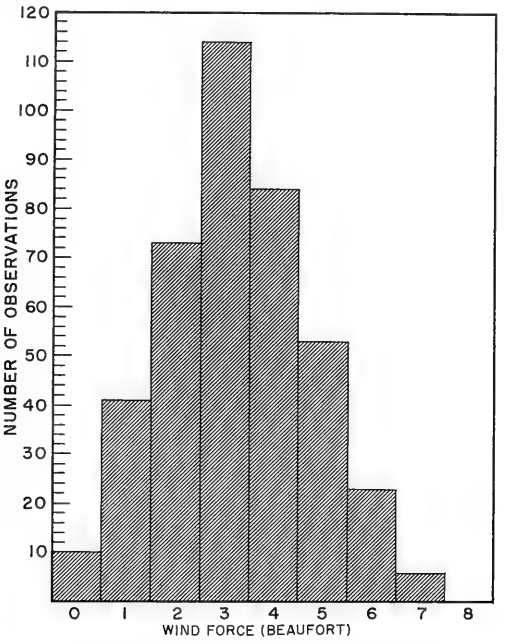

FIGURE 9 FREQUENCY DISTRIBUTION OF WIND FORCE AT OCEAN WEATHER STATION ECHO (35° N, 48° W) IN SEPTEMBER (6 YEARS' DATA, 403 OBS)

There appears to be no semipermanent convergence in the area in spring and early summer, at which time the correlation between mechanical mixing and thermocline depth is approximately the same as at the other Atlantic weather stations.

Knowledge of permanent and semipermanent convergence and divergence in the oceans is limited. Data on currents are scarce and uncertain; therefore, computations of convergence and divergence rates and their effects on the thermocline are not reliable. Monthly statistical computations of existing BT data for at least 5-degree squares would be helpful for detection of permanent or semipermanent convergent or divergent areas and would also be useful for predicting thermocline depth and other properties. Unfortunately, sufficient data for such computations are available only for very limited portions of the oceans.

Mechanical Mixing

With exception of areas of frequent advection as shown in Figure 7, the mixed layer in spring, summer, and early autumn is formed mainly by mechanical mixing. This mechanical mixing is an indirect result of wind stress on the water surface through intermediate action of wind waves and pure wind current.

Little mixing results from orbital motion of particles in regular sinusoidal waves, because mass is not transferred from one level to another. This conclusion is in good agreement with the general observation that swell alone does not appreciably affect the mixed-layer thickness. Only the interaction of several systems of orbital motions, resulting from various origins, dimensions, and directions and with interfering patterns of streamlines, can produce enough turbulence to overcome stability and transfer momentum to adjacent levels. Mixing furnished by wave action can have several causes: (1) interaction of particle motion because of spectral distribution of periods and heights, (2) interaction of orbital particle motion because of angular spreading of wave trains, (3) interaction of orbital motion between surface and internal waves (Figure 10), and (4) breaking wind wave crests. Since the actual process of orbital interaction is not known, all orbital motions may be combined and regarded as orbital turbulence.

Another important agent of mechanical mixing is drift or pure wind current developing at the same time as wind waves. The velocity and vertical extension of this current apparently depend on wind force, fetch, and duration, as do wind waves.

Flow in the ocean is generally considered to be nearly always turbulent; consequently, stirring action is considerably more effective, so that the rate of mixing depends on the rate of flow and the vertical velocity gradient. However, it is doubtful whether a completely mixed surface layer can be formed by an ocean current alone. If total mixing could be caused by horizontal flow, the water would be mixed throughout the vertical extent of permanent currents.

The structure of upper layers in a permanent current is not essentially different from the structure of these layers in areas with little or no horizontal flow. There is a relatively shallow mixed layer and a well-developed thermocline in a permanent current, such as the Gulf Stream,

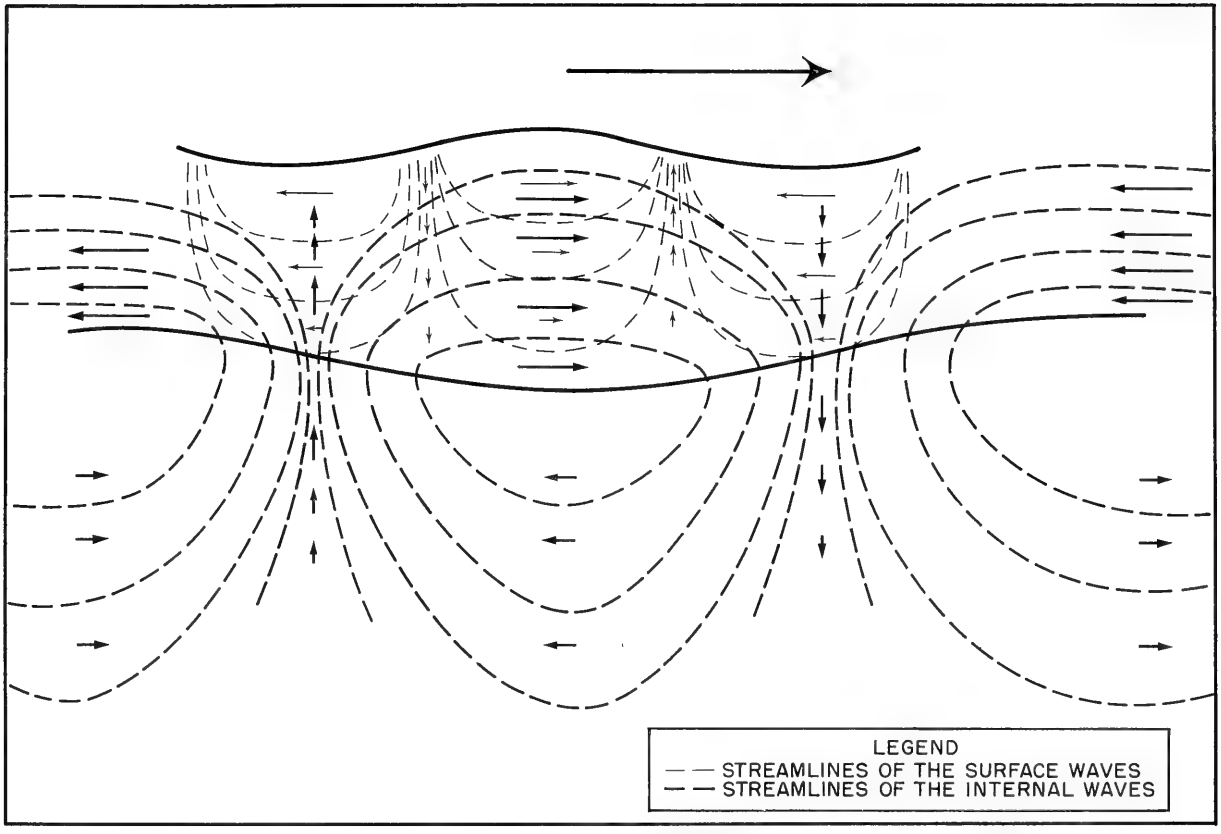

FIGURE IO INTERACTION OF ORBITAL MOTION IN SURFACE AND INTERNAL WAVES

despite this current's vertical extent, which is more than tenfold that of the mixed layer. Although the upper layers in a strong permanent current are more subject to disruptions by advection of "foreign" water masses and are usually less steady than those in a water mass with little or no permanent flow, their formation and structure are similar to those of the latter and follow the same pattern.

It is hardly possible to locate an area of the ocean which does not have horizontal flow extending vertically to a layer of no motion (except at convergence and divergence lines), a level usually located many times deeper than the surface layer of mixed water and the thermocline. For all practical purposes, assumptions can be made that a mixed layer always forms within a moving mass, and that "currents" are only areas or streaks of exceptional velocity of horizontal flow.

Thus, to summarize the factors participating in formation of turbulent motion under given surface conditions at the depth ζ in the mixed layer, the momentum transfer (N) of a mass element in unit time will be the resultant of several component momentum transfers:

$$N = N_o + N_b + N_{wc} + N_{pf} \tag{2}$$

where N_o = component of momentum transfer due to orbital turbulence,
N_b = component of momentum transfer due to breaking crests of surface waves,
N_{wc} = component of momentum transfer due to pure wind current, and
N_{pf} = component of momentum transfer due to permanent flow.

If the mixed layer is in a steady state and the energy produced by surface conditions is insufficient to increase the thermocline depth, any stirring in the mixed layer occurs under neutral conditions. The vertical component of momentum transfer will then be

$$N_z(\zeta) = \rho \overline{V}'_z \overline{l}_z \tag{3}$$

where $\overline{V}'_z$ = mean vertical component of resultant turbulent velocity at the depth ζ and is a function of ζ
$\overline{l}_z$ = mean vertical component of the distance of mass transport at the depth ζ and is also a function of ζ, and ρ is the density.

If surface conditions increase the mixing energy sufficiently to cause an increase in the mixed-layer thickness, mixing occurs in the upper part of the thermocline near the interface; this mixing gradually extends upward to the surface. While stirring continues under nearly neutral conditions in the former mixed layer, stability hampers mixing just below the interface so that the vertical component of the momentum transfer will be

$$N'_z(\zeta) = \frac{\rho \overline{V}'_z \overline{l}_z}{1 + \left(\frac{1}{\rho}\frac{\partial \rho}{\partial z}\right)\overline{l}'_z} \tag{4}$$

where $\bar{l}'_z = \bar{l}_z - \Delta l_z$, a reduced mean vertical component of mixing length due to stability or a vertical distance along which a moving particle is acted upon by the stability.

The vertical component of the momentum transfer at a certain level will decline to such an extent that the downward transfer of heat will not be possible because of the restoring stability force, $-\frac{g}{\rho}\frac{\partial \rho}{\partial z}$. The mixed layer will then be at a new steady state corresponding to existing surface mixing conditions.

Mixing forces all act concurrently; and formation of the mixed layer results from interwoven, inseparable action of all factors. Swell can also participate in mechanical mixing, if the swell is combined with current and wind waves.

Decay of the Mixed Layer

A mixed surface layer of given age and depth has a limited area. Age is defined as the number of days expiring after mechanical mixing ceases. Assume that a mass of homogeneous water exists to a certain depth over a certain area. Outside this area the surface mixed layer has different properties. The homogeneous body of water floats within or above a system of nonhomogeneous water which has inherent characteristics of motion. The depth of the moving nonhomogeneous water is considerably greater than that of the mixed layer. The thermocline is therefore a part of the surrounding nonhomogeneous system. The water of the mixed surface system is not required to be completely homogeneous horizontally, because it can extend over several nonhomogeneous systems. The mixed-layer system is characterized mainly by pure wind current and wind waves that have acted to produce the mixed layer over the specific area of the wind field.

In the absence of a mixed layer, the nonhomogeneous system may be assumed to extend from the surface to the bottom or to a layer of no motion as shown in Figure 11A. After a mixed layer has been formed over a wind field, the mean flow of pure wind current in the mixed layer will be approximately at right angles to the wind and at a certain angle to the mean direction of flow of the nonhomogeneous system, as shown by arrows in Figure 11B (when wind direction is toward the observer).

After the mixing process ceases, the mixed layer possesses no kinetic energy. The mixed layer will then be absorbed by the nonhomogeneous system. The process of transformation is probably quite complex; however, a few distinct partial processes may be assumed. Firstly, the whole mass of mixed water should undergo deformation due to loss of dynamic rigidity gained during mixing from independent horizontal flow and eddy viscosity. The entire mixed layer becomes elongated and flattened during adaptation to the permanent flow. In this process, velocity of currents in the thermocline is gradually imparted to the mixed layer (Figure 12). Secondly, the permanent flow in the upper part of the thermocline is not sufficient to produce a complete mixed layer but is strong enough to accelerate temperature conduction which extends the temperature gradient into the lower

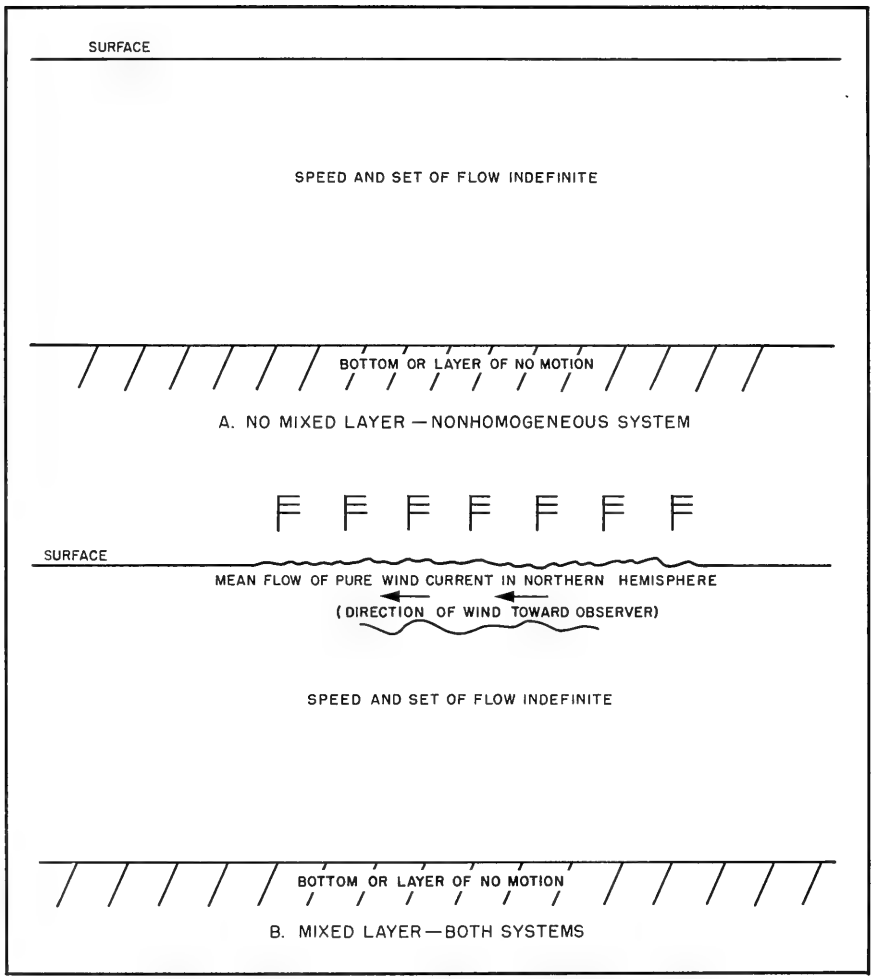

FIGURE 11 HOMOGENEOUS AND NONHOMOGENEOUS SYSTEMS

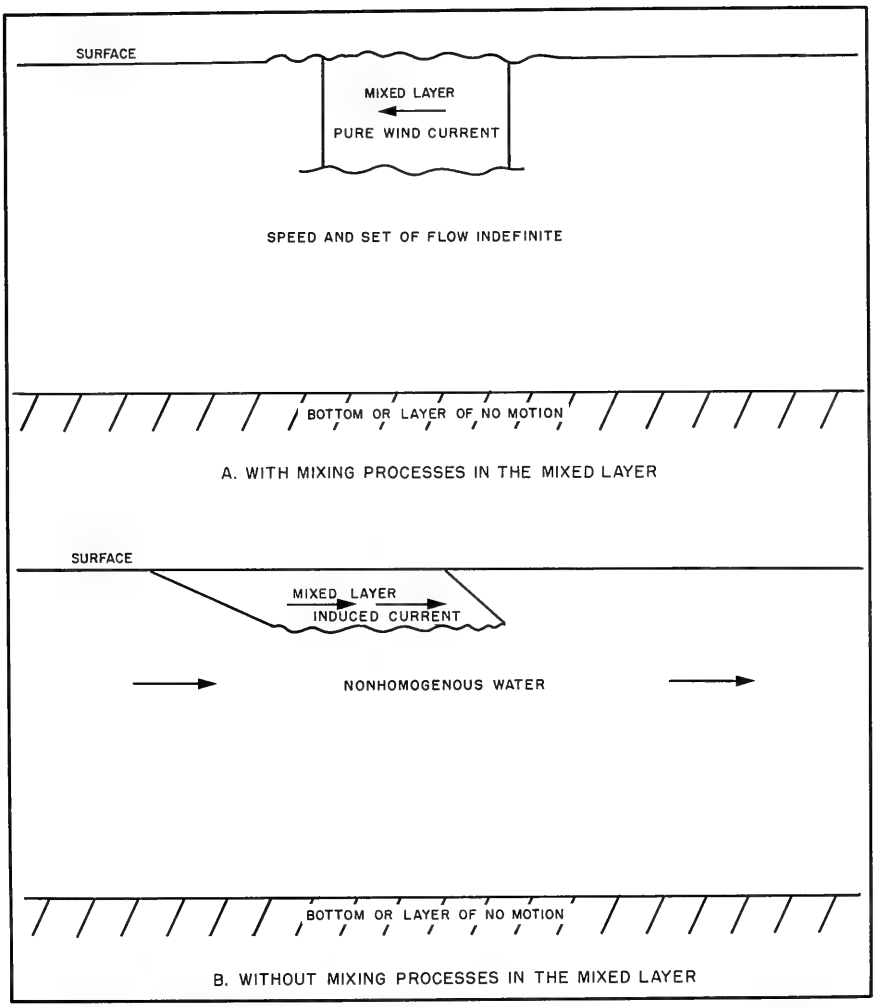

FIGURE 12 DEFORMATION OF THE MIXED LAYER BY INDUCTION OF VELOCITY FROM SURROUNDING NONHOMOGENEOUS WATER

part of the mixed layer. Equation (2) is now equal to or nearly equal to zero in the mixed layer:

$$N_o + N_b + N_{wc} + N_{pf} = 0$$

The fourth and perhaps the first terms continue to exist below the area of interface. The term N_o is not completely equal to zero in the presence of internal waves. Of the spectrum of orbital motions existing during mixing, the portion due to internal waves remains and may interact with the horizontal flow in the thermocline, thus maintaining mixing in the region of the interface.

When the mixing process in the mixed layer ceases, the layer should begin to decay immediately. The depth of the thermocline at any age should be inversely proportional to the age τ (in days), inversely proportional to the mean horizontal velocity $\bar{V}$ in the thermocline, directly proportional to the thickness h of the mixed layer at the steady state, and directly proportional to the length L (in miles) of the mixed field. An expression for thermocline depth h_τ at any age, combining all the involved factors, is:

$$h_\tau = \frac{K}{\tau \bar{V}} hL \qquad (5)$$

where K is a proportionality factor.

K could be determined empirically, if the other five quantities in Equation (5) were known or could be easily measured. However, usefulness of this equation would be very limited, even if K could be determined. Such a simple situation seldom occurs in the oceans. For example, if the wind stopped abruptly over a fully developed sea which had previously been subjected to a wind field of 30 knots and in which the thermocline depth was in a steady state, aging of the mixed layer would begin as soon as the sea surface became almost calm and the pure wind current had stopped completely. If the calm condition continued, Equation (5) would apply.

As a second example, if a fully developed sea with given stability in the thermocline and a wind field of 30 knots are assumed, the mixed layer would maintain a thickness of 120 feet. Then suppose the wind field diminishes to 20 knots and continues to blow indefinitely in the same direction; the wind wave spectrum will gradually conform to the reduced wind condition, and turbulence in the mixed layer will accordingly be weaker; however, mixing will continue under neutral conditions to 120 feet. Under wind conditions of 30 knots, turbulence in the region of the interface can penetrate no deeper, because it is arrested by thermocline stability; but since the mixing reaches considerably deeper under neutral or nearly neutral conditions and given wind conditions, turbulence produced by a wind of 20 knots may be sufficient to resist detrition at the interface and deformation of the existing mixed layer to 120 feet. In such circumstances decay would be prevented, and the mixed layer previously formed by turbulence caused by 30-knot winds would continue to exist as long as the turbulence produced by weaker surface conditions was

able to balance the detrition and deformation forces. This balancing requires considerably less energy than is required to overcome stability; consequently, deepening of the thermocline can occur only with adequate surface conditions, whereas the mixed-layer thickness can be maintained by weaker surface conditions.

Since actual conditions in the oceans are generally similar to those given in the second example, there are additional problems of determining how much the mixing energy must decrease before decay can begin, and how far and at what rate the decay will proceed once it begins. Convergence must also be considered with respect to decay. On the convergent side of the field of pure wind current, another current following the wind direction results from piling up of the water. This current will continue to flow after the pure wind current ceases and will also tend to maintain the already developed mixed layer, thus delaying its decay.

In general, decay is quite rapid in strong permanent currents. Effects may be observed in periods as small as one day. In areas of very slow geostrophic flow, decay is also slow; and the age of a few days may reveal no marked effects.

All considerations lead to the conclusion that prediction of the thermocline depth cannot always be based on the wind field in an area. The history of surface conditions for approximately 15 to 20 preceding days must be taken into consideration, and the prediction must be based on the most recent and strongest mixing conditions.

At present, historical data are inadequate for more efficient formulation of the decay and time lag problems. Since the decay process is closely related to motion below the interface between the mixed layer and the thermocline, regional and seasonal peculiarities have great importance. Personal experience of a forecaster may be greatly helpful in certain areas during certain seasons.

PROCEDURE

Determination of the Mixing Parameter

In the absence of mixing by instability or by permanent convergence or divergence, existence of the mixed layer is attributable to a complex process of mechanical mixing. Water particles are interchanged between the surface and bottom of the mixed layer by energy supplied in varying amounts from various origins. Turbulent motion of a particle is the resultant of several simultaneous component forces acting in different proportions.

The main mechanical mixing factors are derived from wind stress on the water. Either wind or a combination of wind waves and pure wind current may be used to correlate the thermocline depth with its causes. The

amount of turbulence depends on the dimensions of the turbulent field as considered in the formula for the Reynolds number,

$$R = \frac{\rho u L}{\mu}$$

where ρ is density,
u is horizontal velocity of flow,
L is linear extension of flow, and
μ is the coefficient of viscosity.

In stirring processes more complex and effective than pure horizontal flow, the duration of wind stress must also be taken into account. By choosing the wave parameters, fetch and duration are introduced automatically--their part in wave development is relatively well known.

The velocity and vertical extension of pure wind current also depend on the fetch and duration of the wind and can be assumed to be proportional to the dimensions of spectral components of the wind sea. If only wave parameters are used for determination of the mixing parameter, the pure wind current factors may be considered as having been incorporated in the mixing parameter. The problem is thus simplified sufficiently to permit experimentation in determination and prediction of the mixed-layer thickness.

Wave height or amplitude, period, length, and steepness are expected to contribute to the problem. Length and period are naturally interdependent; therefore, only one of these must be considered. Spectral distribution of steepness in a wind sea is difficult to determine; however, it is a function of the spectral distribution of height and length and is therefore partly accounted for by use of these parameters.

The mixed-layer thickness is finally considered to be a function of wave amplitude A, wave length λ, and a mixing parameter k, $h = f(A,\lambda,k)$, which is valid at the interface between the mixed layer and the thermocline. k cannot be expected to remain constant. Since it applies to the bottom of the mixed layer, it must be dependent on mixed-layer thickness and on the wave parameters. In addition, its value depends on the stability in the thermocline.

The relation describing orbital motion in trochoid waves

$$k = A e^{-\frac{2\pi h}{\lambda}} \qquad (6)$$

includes most of the parameters, if h is considered to be a fixed value under given surface conditions and if stability in the thermocline is constant. The above function, $k(A,h,\lambda)$, was adopted in view of the generally accepted theory that orbital motion of particles due to waves and the velocity of the pure wind current both decrease exponentially with depth and are proportional to the wave parameters.

The mixing parameter k is proportional to $\overline{l_z'}$ in Equation (4) and can be interpreted as the length of momentum transfer at the bottom of the mixed layer, when the momentum transfer is reduced so much that the restoring force of stability is sufficiently strong to prevent further turbulent heat conduction across the interface.

Solving (6) for h gives

$$h = \frac{\lambda}{2\pi} \ln\left(\frac{A}{k}\right) \qquad (7)$$

Equation (7) can be used to compute h, if the wave parameters and the corresponding value of k for existing stability in the thermocline are known.

Wave Parameters

A total of 356 k values have been determined with known mean thermocline depth and known wave parameters. These values were computed over a large range of stabilities and wave spectra. The total wave spectrum cannot be applied in Equation (7), owing to the complexities involved. Certain wave heights and lengths are assigned as being characteristic of given spectra. Significant wave height ($H_{1/3}$), the mean of the highest one-third of the waves, was determined by the Pierson-Neumann-James method. An amplitude equal to one-half of the significant wave height was then used in Equation (6) for determination of k. Wave length was computed by the relation $\lambda = 3.41\ T_{max}$, where T_{max} is the period of maximum energy of the spectrum for a fully developed sea. When the sea was not fully developed, significant height was determined accordingly, and the period of maximum energy corresponding to that significant height for a fully developed sea was used. When this period exceeded the maximum period possible for a given non-fully developed sea, the latter period was applied. As a rule, the wave parameters of a fully developed sea were used for determination of k values; only a few determinations were made for a non-fully developed sea, in which applicability of the method is not too certain.

In use of Equation (7) for prediction of the thermocline depth, the same characteristic elements of the sea spectrum ($A = 1/2\ \overline{H}_{1/3}$ and $\lambda = 3.41\ T^2_{max}$) must be considered. If other representative elements of the spectrum were used, such as mean height and mean period, a different set of k values would apply.

In summary, k values apply in Equation (7) in this study only with significant wave heights and wave lengths computed with periods of maximum energy of the spectra.

Stability

Stability, generally defined as $E = \frac{1}{\rho}\frac{\partial \rho}{\partial z}$, is a function of temperature and salinity distribution, $E\left(\frac{\partial T}{\partial z}, \frac{\partial S}{\partial z}\right)$. A BT shows only the temperature distribution and does not obtain simultaneous salinity determination.

In general, data concerning salinity distribution in the thermocline are extremely scarce. Several random samples of salinity distribution in the thermocline in the area around OWS CHARLIE show that the salinity gradient is rather small, and that it probably does not vary much with time. As a first step in this study, only the temperature gradient was considered to be a stability factor; salinity was assumed to be constant. Neglect of salinity variation in time and space involves certain error; however, other difficulties are also inherent to this problem.

Temperature gradients obtained from BT data are only instantaneous values, whereas considerable continuous variation of this gradient occurs in the thermocline. Variation of the gradient is dependent mainly on internal waves at the top and bottom of the thermocline, so that only a mean value of the gradient can be practically applied for a given location and for a given time period. Variance of several monthly means depends on properties of internal waves which are more elusive and more difficult to determine, rather than on the actual temperature distribution in the thermocline. The mean value for a given location and for a given month in one year can be quite different from that for the same location and the same month in another year, because amplitudes and phases of internal waves at the upper and lower boundaries of the thermocline are different (Figures 2, 5, and 6).

On the assumption that the vertical temperature difference is proportional to the mean temperature gradient in the upper part of the thermocline, the difference in the entire thermocline was adopted as the index of stability instead of the temperature gradient in the upper part of the thermocline. Since the temperature gradients in the mixed layer and below the thermocline are small, computation of the temperature difference between the surface and a level below the seasonal thermocline is more convenient. The 500-foot level would probably be most convenient. BT's usually reach a depth of only 400 feet; therefore, values at this level were used for computing $\overline{\Delta t} = (\overline{T}_o - \overline{T}_{400})$. Mean temperature difference is more easily determined than the mean temperature gradient in the thermocline and apparently reflects more stability with respect to yearly oscillations.

Figure 13 shows frequency distributions, means, and standard deviations of (1) temperature difference (Δt) between the surface and 400 feet, (2) temperature at 400 feet, and (3) temperature gradient (G_t) per foot in the thermocline computed from observations made at OWS CHARLIE between 7 and 22 September 1960. BT's were made every half hour when possible. Owing to operational requirements of the observing ship, observations were interrupted for one or more hours a few times each day; there were also a few longer interruptions due to heavy storms.

Figure 14 shows frequency distributions and means of temperature difference (Δt) between the surface and 400 feet and temperature gradient per foot in the thermocline computed from BT's taken every 5 minutes for eight one-hour periods during the same period mentioned above. These observations were not used in Figure 13.

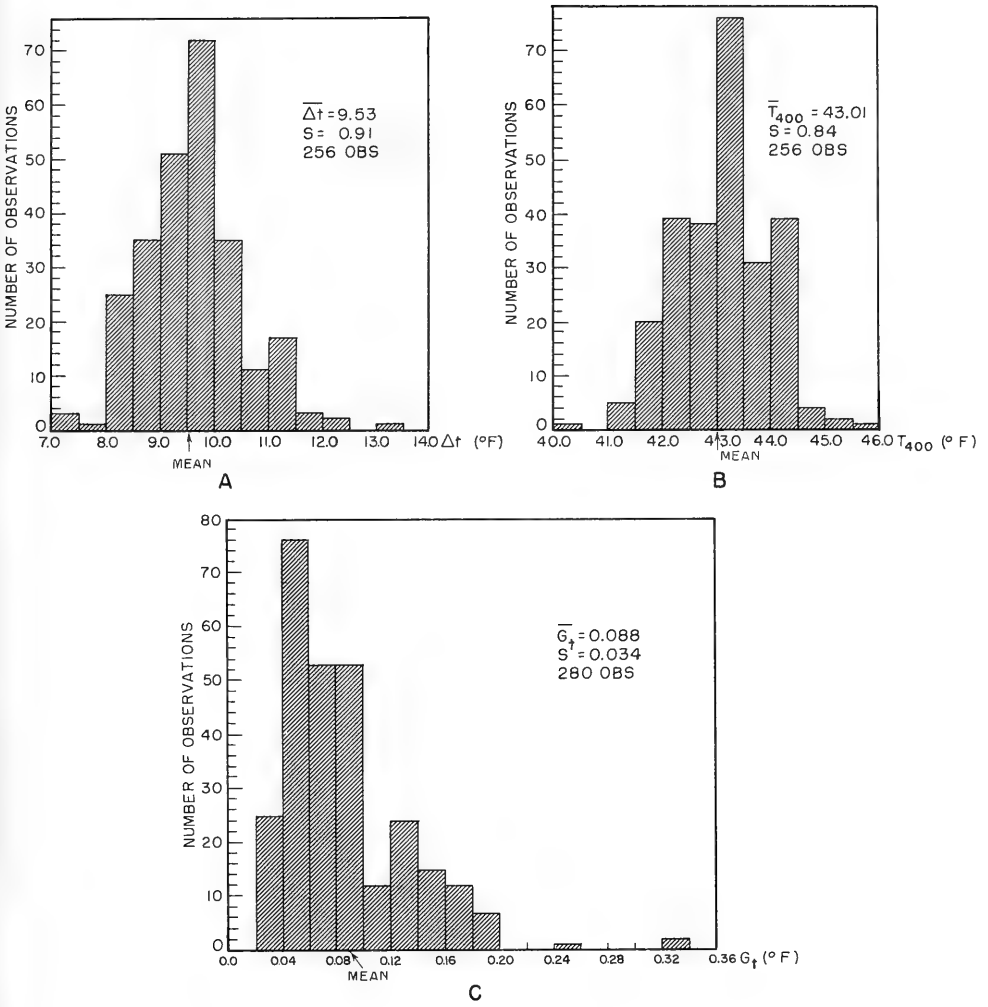

FIGURE 13 FREQUENCY DISTRIBUTIONS, MEANS, AND STANDARD DEVIATIONS OF Δt, TEMPERATURE AT 400 FEET, AND TEMPERATURE GRADIENT (G_t) PER FOOT IN THE THERMOCLINE BASED ON HALF-HOURLY BT'S

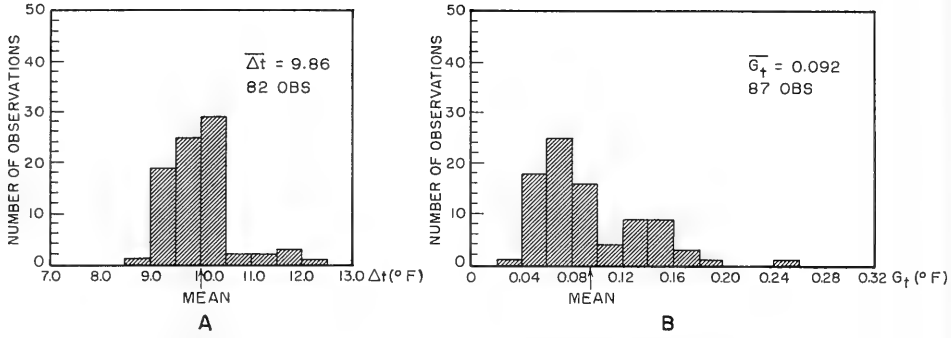

FIGURE 14 FREQUENCY DISTRIBUTIONS AND MEANS OF Δt AND TEMPERATURE GRADIENT (G_t) PER FOOT IN THE THERMOCLINE BASED ON BT'S TAKEN EVERY 5 MINUTES FOR 8 ONE-HOUR INTERVALS

In both cases Δt values are more evenly distributed about the mean than are gradient values. Use of the 500-foot reference level for Δt instead of the 400-foot level would certainly show a considerably narrower band of oscillation. In either case, application of the temperature gradient rather than temperature difference would not be more advantageous from the point of view of constancy.

Temperature gradient oscillations in the thermocline can be expected to increase the mixing rate when the gradient is small and to decrease it when the gradient is large. Oscillations in the upper part of the thermocline do not occur evenly over a large area but follow the spectral distribution of the internal wave systems at the top and bottom of the thermocline. The mixing process may be very effective in some small areas because of decreased stability in the thermocline and may be arrested in other areas by increased stability. The overall situation is constantly changing; however, this unevenly distributed mixing process may affect the spectral distribution of the internal waves at the interface between the mixed layer and the thermocline.

The mean temperature gradient in the thermocline depends on the mean stability index $\overline{\Delta t}$ and on the thickness of the thermocline which, to a certain extent, is inversely proportional to the mixed-layer thickness. Increase of the mixed-layer thickness decreases the thermocline thickness and increases the temperature gradient in the thermocline, if $\overline{\Delta t}$ is nearly constant. However, decrease of the thermocline thickness with increasing mixed-layer thickness is not linear, because the bottom of the seasonal thermocline tends to move downward as the top of the thermocline moves downward. Downward movement of the bottom is considerably smaller and possesses a certain time lag in relation to downward movement of the top. When the top of the thermocline rises, the mixed-layer thickness decreases, and the bottom of the thermocline also rises.

A certain initial stability exists with a given $\overline{\Delta t}$ in the absence of a mixed layer. If the mean stability index remains constant, stability increases from the initial value with increasing mixed-layer thickness. Increase of stability is slow when the mixed layer begins to form and gradually becomes greater as the mixed-layer thickness and Δt increase. Table 2 lists mixing parameters (k) for various stability indexes before mixing begins. These values apply during initial formation of the mixed layer near the surface. In Figures 15 through 22 these k values are at the point where $k(\eta) = 0$ and $\overline{h}(k) = 0$.

TABLE 2

k VALUES AT INITIAL STABILITY

Stability index Δt(°F)		k	Stability index Δt(°F)		k
2°	(0°-4°)	0.10	11°	(10°-12°)	0.21
5°	(4°-6°)	0.13	13°	(12°-14°)	0.24
7°	(6°-8°)	0.16	15°	(14°-16°)	0.27
9°	(8°-10°)	0.19	17°	(16°-18°)	0.30

η Curves

To connect mixing parameter values with stability and wave parameters, another parameter $\eta = HT$ was introduced. $H_{1/3}$ is significant wave height, and T_{max} is the period of maximum energy of the spectrum. η is used as a measure of sea state for wind waves. k values determined in Equation (6) with known wave parameters and mean mixed-layer thickness ($\overline{h}$) values were plotted against η values computed with corresponding wave parameters for eight groups of Δt. The resulting distribution of points suggests a parabolic law. Curves computed for each Δt group with the equation

$$\eta^2 = 2p\,(k-k') \tag{8}$$

readily fit the distribution of points. k' in (8) is the value of the mixing parameter at initial stability with the given Δt, and

$$p = \frac{\Sigma\, \eta^2\,(k-k')}{2\,\Sigma\,(k-k')^2}$$

determined by the least square method.

p values for stability index intervals from 0° to 18° F are shown in Table 3.

TABLE 3

p VALUES FOR VARIOUS STABILITY INDEX GROUPS

Stability index $\Delta t(^{o}F)$	p	Stability index $\Delta t(^{o}F)$	p
2^{o} $(0^{o}\text{-}4^{o})$	108.2×10^{3}	11^{o} $(10^{o}\text{-}12^{o})$	17.2×10^{3}
5^{o} $(4^{o}\text{-}6^{o})$	42.8×10^{3}	13^{o} $(12^{o}\text{-}14^{o})$	13.3×10^{3}
7^{o} $(6^{o}\text{-}8^{o})$	28.7×10^{3}	15^{o} $(14^{o}\text{-}16^{o})$	10.3×10^{3}
9^{o} $(8^{o}\text{-}10^{o})$	22.2×10^{3}	17^{o} $(16^{o}\text{-}18^{o})$	8.0×10^{3}

Computed p values are assumed to correspond closely to the representative values of Δt for each Δt interval. The normal η curves in Figures 15 through 22 are plotted with these values of p. The normal η curve for the Δt interval of 0^{o} to 4^{o} is a very open parabola. As stability indexes increase, η curves aline downward in a rather regular way so that increase of the stability index by one degree Fahrenheit results in the ratio $\frac{p_{n+1}}{p_n}$, where n is the stability index in whole degrees. For stability indexes between 1^{o} and 7^{o} F this ratio increases by a constant amount for each degree Fahrenheit as follows:

$$\frac{p_2}{p_1} = 0.6 + 0.04, \quad \frac{p_3}{p_2} = 0.6 + 2(0.04) \ldots \quad \frac{p_{n+1}}{p_n} = 0.6 + n(0.04)$$

For Δt of 1^{o} F, p is 179.4×10^{3}. The equation for computation of subsequent η curves is

$$\eta_{\Delta t=n+1} = \left[2p_{\Delta t=n} \, (0.6+0.04)(k-k'_{n+1}) \right]^{1/2} \tag{9}$$

For Δt equal to 7^{o} and more, the ratio $\frac{p_{n+1}}{p_n}$ becomes constant and is 0.88. Equation (9) then becomes

$$\eta_{\Delta t=n+1} = \left[1.76p_{\Delta t=n} \, (k-k'_{n+1}) \right]^{1/2} \tag{10}$$

The value of p, 108.2×10^{3}, obtained from the distribution of points and applied to compute the normal η curve for the Δt interval of 0^{o} to 4^{o} F does not correspond exactly to the value obtained from the law of p ratios for Δt of 2^{o}. It corresponds to a value which is slightly higher, approximately 2.13^{o} F. This is quite understandable, because samples close to Δt of 0^{o} are neglected in computing k values, and the representative mean value for this interval is slightly greater than the median.

Convergence and Divergence

If the wind field remains stationary for a period of time or is propagating slowly enough to produce fully developed or nearly fully developed sea, the pure wind current associated with the wind field should create areas of convergence and divergence. However, the problem is quite complex.

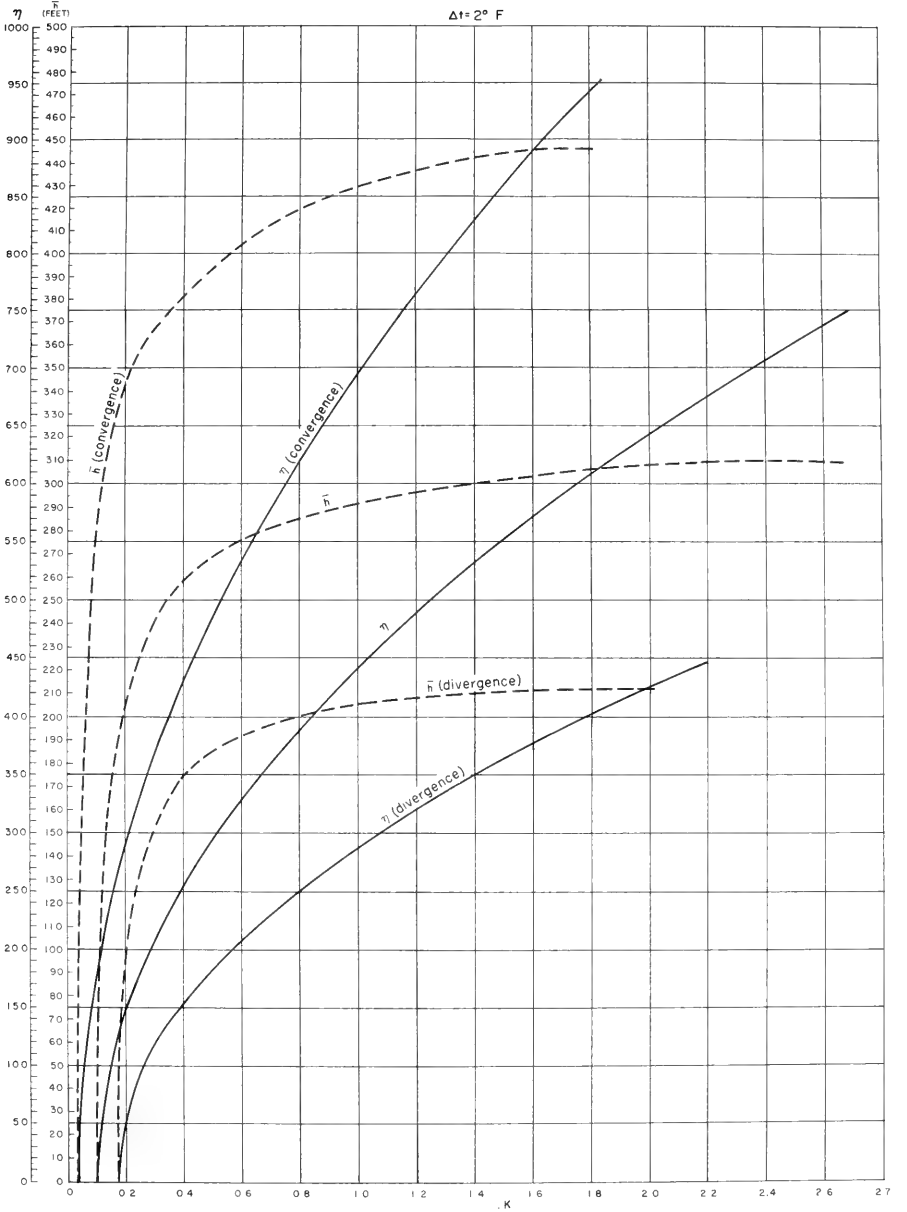

FIGURE 15 PARAMETERS η AND $\bar{h}$ VERSUS k FOR STABILITY INDEX Δt = 0° TO 4° F

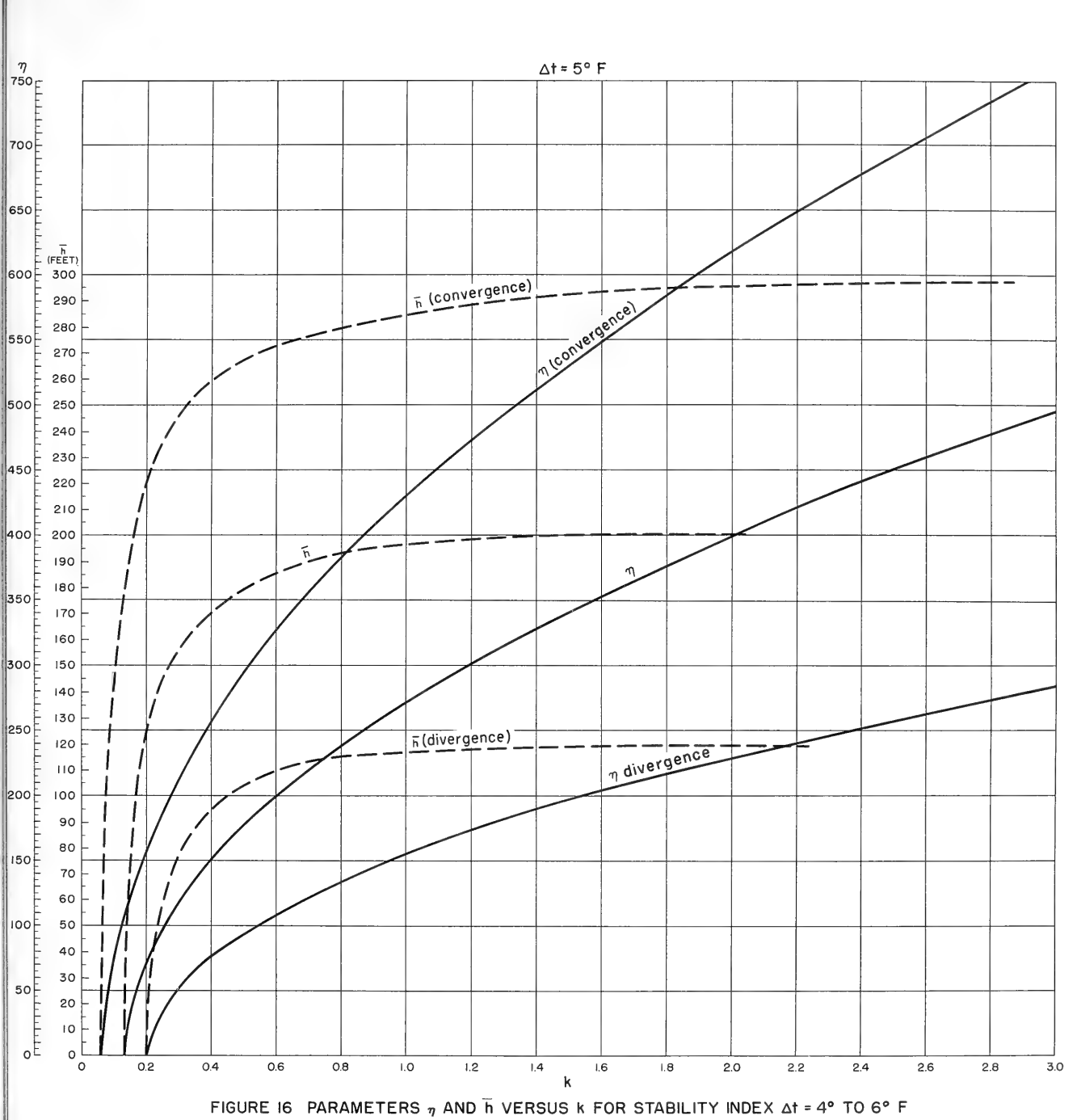

FIGURE 16 PARAMETERS η AND $\bar{h}$ VERSUS k FOR STABILITY INDEX Δt = 4° TO 6° F

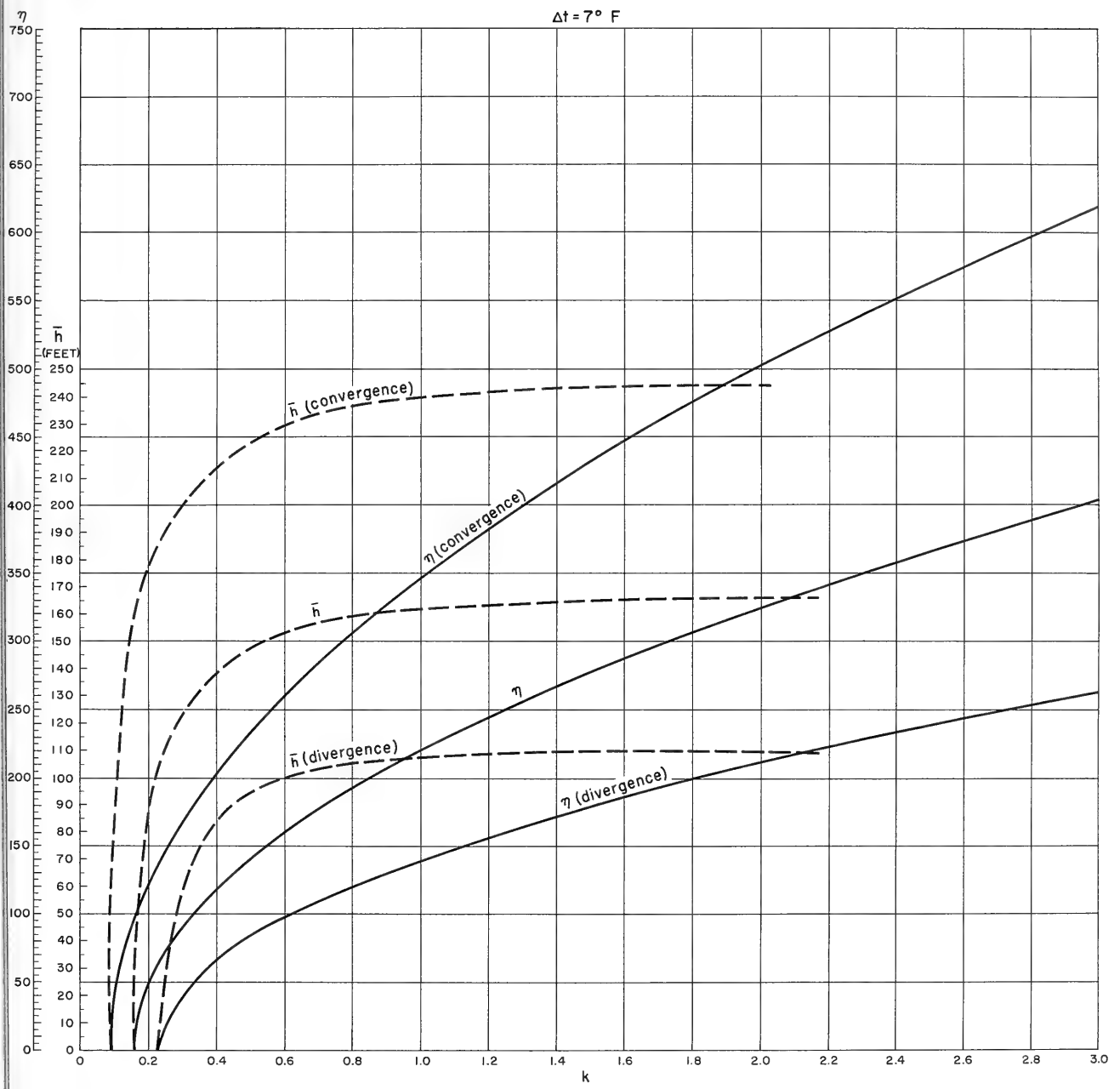

FIGURE 17 PARAMETERS η AND $\bar{h}$ VERSUS k FOR STABILITY INDEX $\Delta t = 6°$ TO $8°$ F

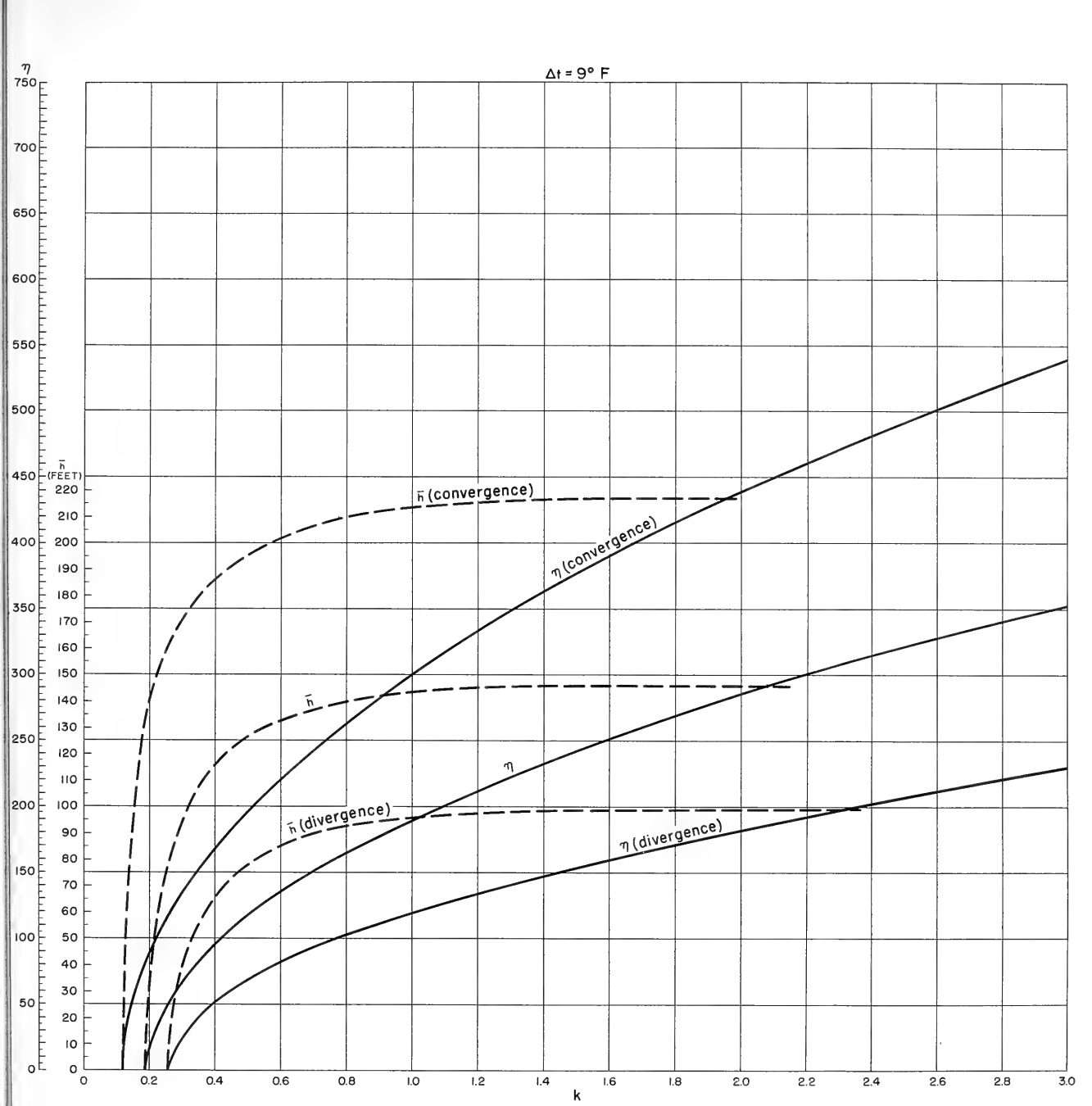

FIGURE 18 PARAMETERS η AND $\bar{h}$ VERSUS k FOR STABILITY INDEX Δt = 8° TO 10° F

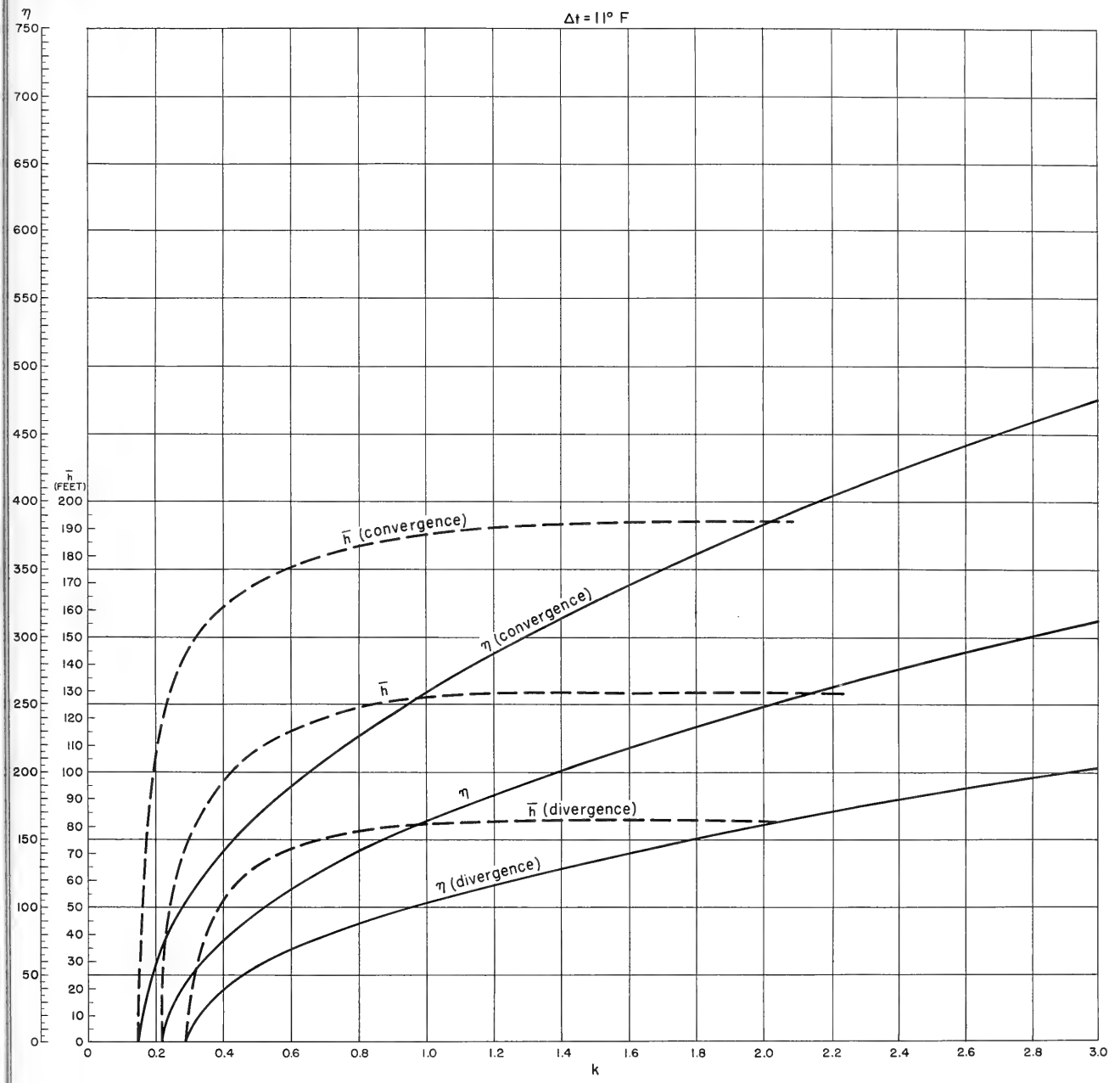

FIGURE 19 PARAMETERS η AND $\bar{h}$ VERSUS k FOR STABILITY INDEX Δt = 10° TO 12° F

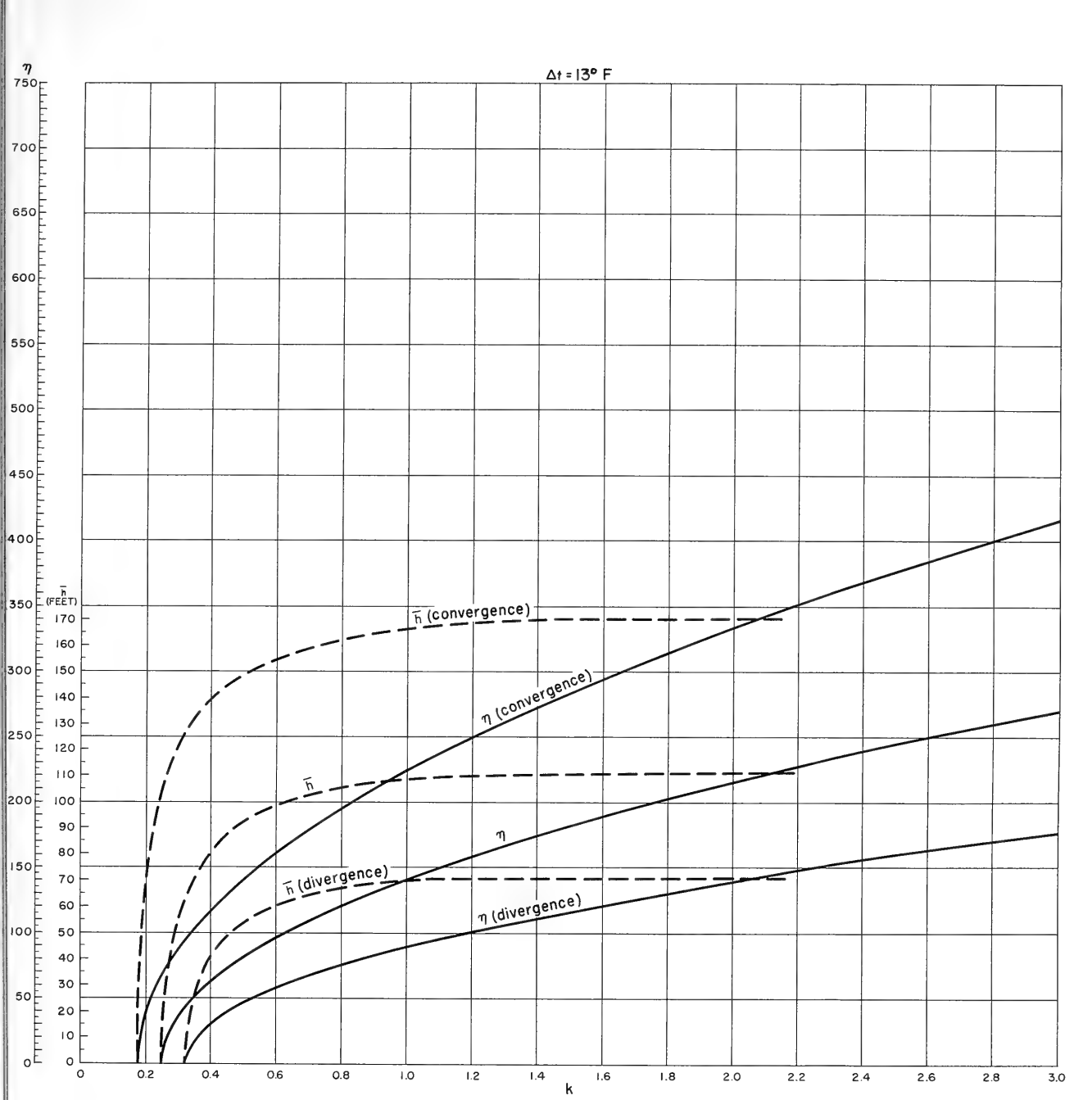

FIGURE 20 PARAMETERS η AND $\bar{h}$ VERSUS k FOR STABILITY INDEX Δt = 12° TO 14° F

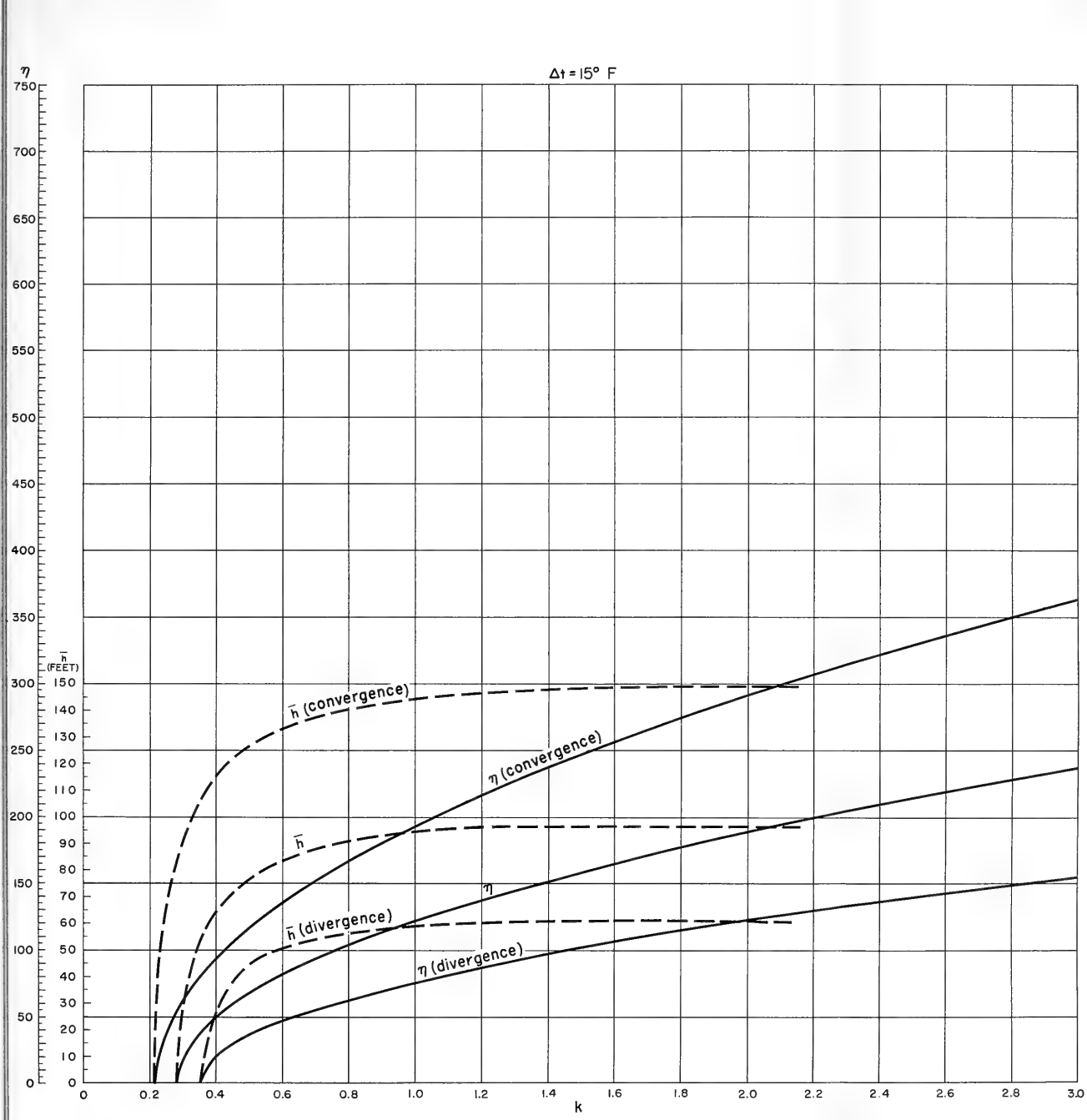

FIGURE 21 PARAMETERS η AND $\bar{h}$ VERSUS k FOR STABILITY INDEX Δt = 14° TO 16° F

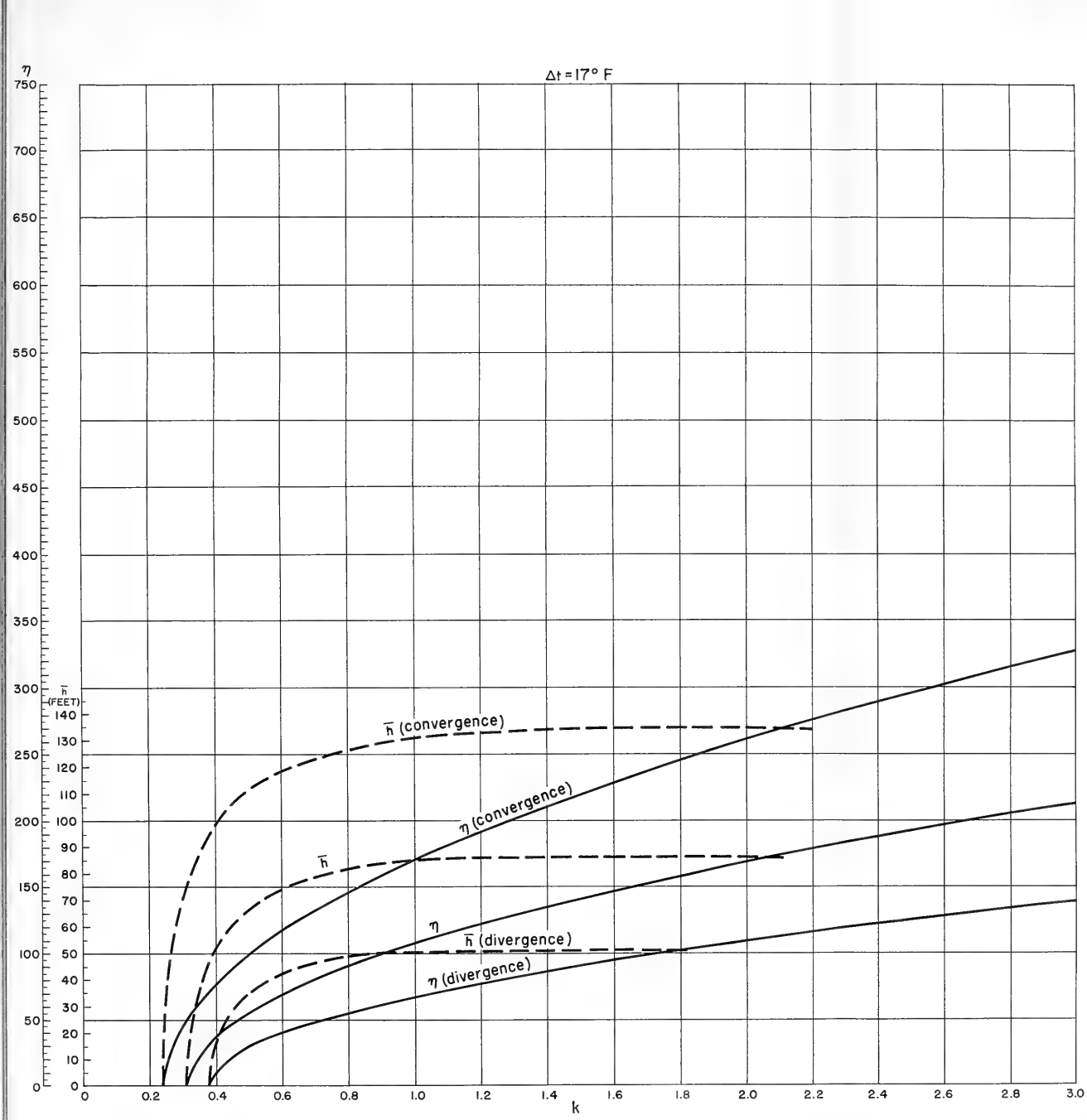

FIGURE 22 PARAMETERS η AND $\bar{h}$ VERSUS k FOR STABILITY INDEX Δt = 16° TO 18° F

Direction and velocity, their changes with depth, and the mean mass transport of a pure wind current are very uncertain; consequently, locations and rates of convergence and divergence are even more difficult to determine. Permanent dynamic factors undoubtedly exert considerable influence on vertical motion of water produced by a transitory wind field and may strengthen, reduce, or even destroy convergence or divergence rates, thereby masking convergence or divergence in areas where it might usually be expected.

The vertical component of motion in an area of convergence increases mixing energy, resulting in an increase of the mixed-layer thickness. Rise of the thermocline and a dome-shaped conformation of isopycnal surfaces in an area of divergence are due to upwelling.

k values were determined by means of Equation (6) using known mean mixed-layer thickness and wave parameters. Plotting of these values against the sea state parameter η for given Δt intervals revealed anomalous deviation of some points: some deviated upward; others, downward (Figure 23). These points could generally be identified with areas that suggest convergence or divergence with respect to the distribution of high and low pressure areas, and their associated wind fields. Figures 24 and 25 show typical examples of areas assumed to be convergent or divergent. Most scattered points of $k(\eta)$ usually coincide with such areas; however, effects of convergence or divergence are not always evident.

Increase of mixed-layer thickness due to convergence occurs most often at the rear of a slowly propagating cyclonic field (Figures 24 and 25). Strong convergence may develop between two cyclonic areas as shown in Figure 25B. A convergence effect also usually develops at the center of a high (Figure 24B). In general, convergence is stronger when pure wind current counters the permanent flow; convergence may not occur if direction of the pure wind current coincides with that of the permanent flow. In contrast, divergence usually occurs at the center of a low or at a slowly propagating front where wind direction changes sharply, as shown in Figures 24A and 24B. In general, divergent conditions are more difficult to determine or justify by existing distribution of the wind field than are convergent conditions.

Each ocean area (some of which are perhaps 5 degrees or less square) possesses individual geographic characteristics which affect formation of the mixed layer and thermocline. In some cases, such as in areas of permanent convergence or divergence, these characteristics may be sufficiently strong to preclude conventional mixing processes. Beyond such extreme cases, local effects are assumed as always present in some degree, acting in different proportions and ways from one area to another. Local conditions seem to be especially effective on mixed-layer changes due to convergence or divergence. Actually, local factors probably exert initial influence on convergence and divergence resulting in a chain effect on the mixed layer.

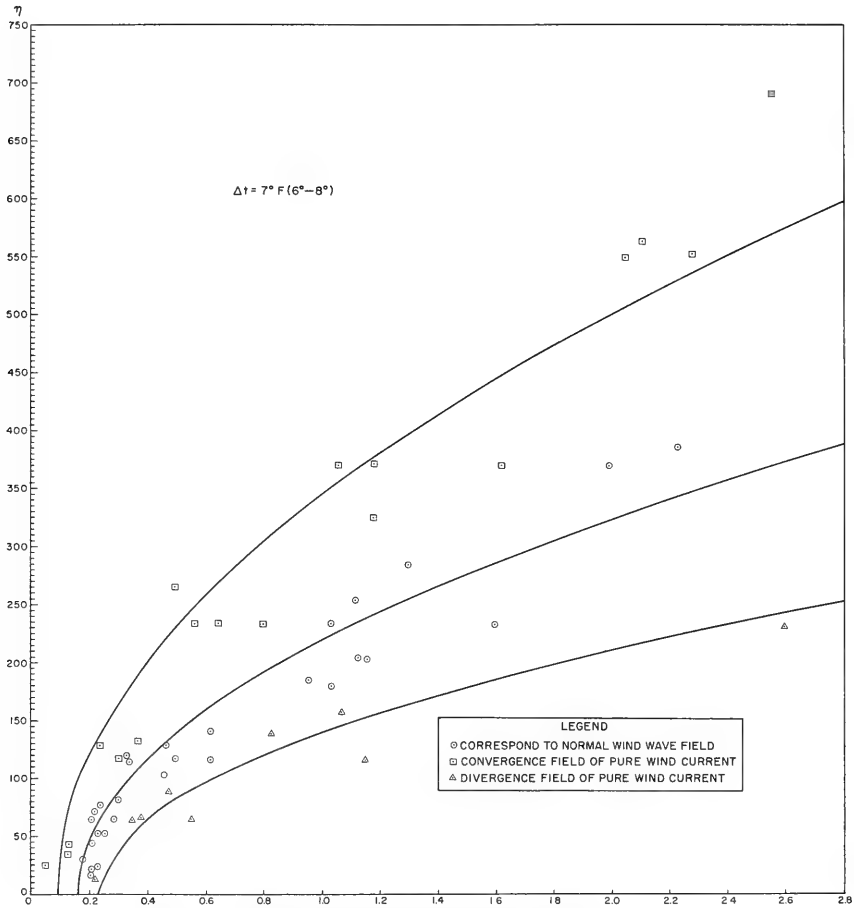

FIGURE 23 EMPIRICAL POINTS OF K VERSUS η FOR Δt = 6°–8° F

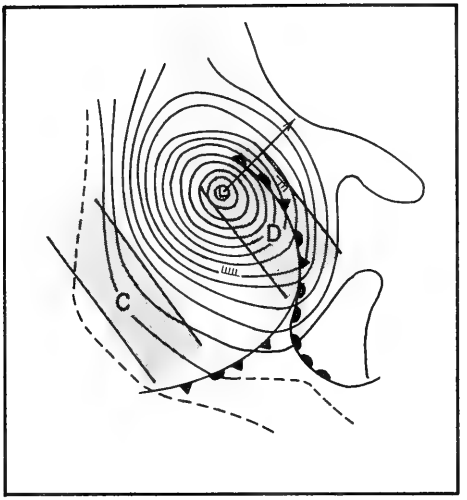

A

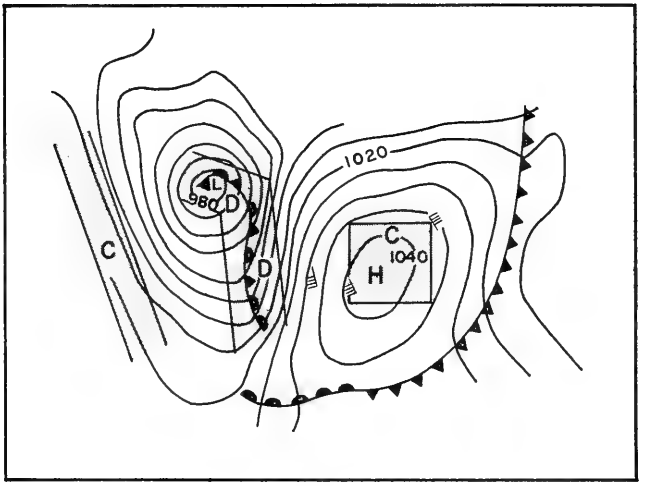

B

FIGURE 24 RELATIONSHIP OF TYPICAL ASSUMED CONVERGENT AND DIVERGENT FIELDS AS APPLIED TO PRESSURE SYSTEMS FOR CHOICE OF η CURVES
(C = CONVERGENCE, D = DIVERGENCE)

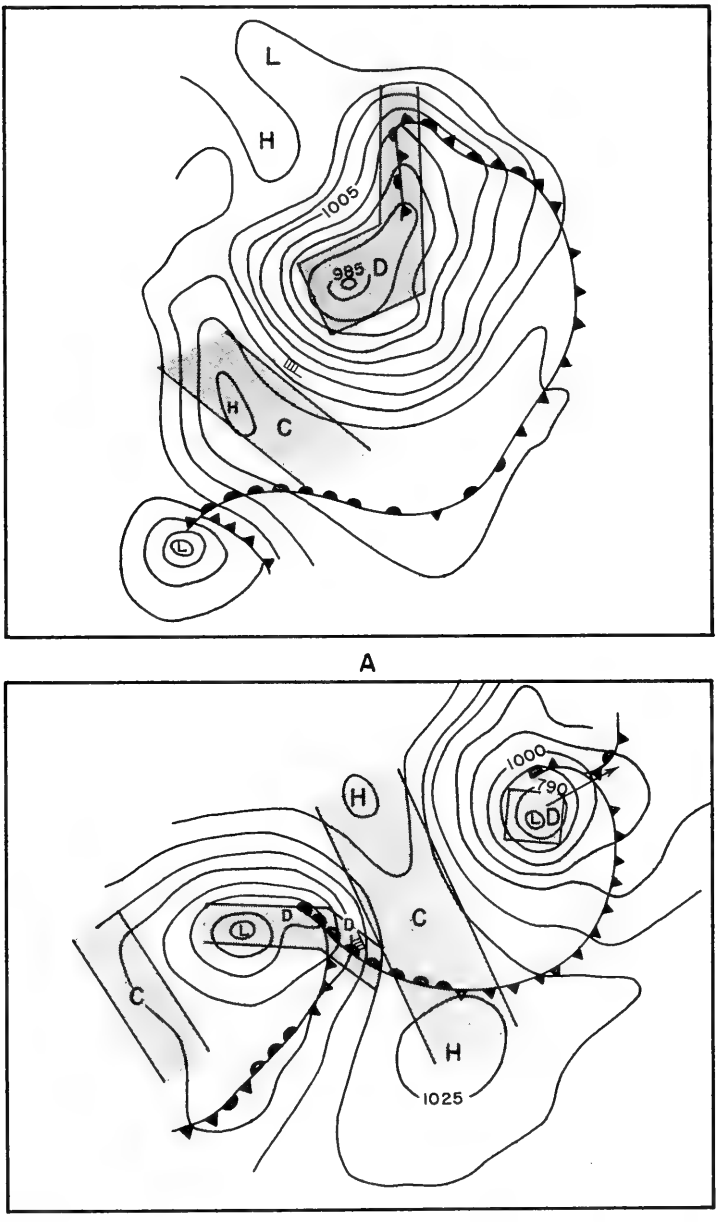

FIGURE 25 RELATIONSHIP OF TYPICAL ASSUMED CONVERGENT AND DIVERGENT FIELDS AS APPLIED TO PRESSURE SYSTEMS FOR CHOICE OF η CURVES (C = CONVERGENCE, D = DIVERGENCE)

Figure 23 shows the distribution of three types of points of k (η) for the Δt interval of 6° to 8° F. The upper points, designated by square symbols, correspond to convergent conditions; central points (circles) are normal values in the wind field with horizontal flow of pure wind current; and the lower group (triangles) correspond to divergence areas. Each group of points follows the same functional pattern and spreads from the central (normal) group increasingly with k and η. The same pattern occurs in all Δt intervals. Largest p values for all 3 groups of points lie in the Δt interval of 0° to 4° F, and smallest p values for all 3 groups lie in the Δt interval of 16° to 18° F.

p values computed for convergence and divergence curves by least squares for all available Δt intervals show a certain variation of the ratios $\frac{p_{norm}}{p_{conv}}$ and $\frac{p_{div}}{p_{norm}}$ within each interval. This variation is probably due to sparsity of data. The total range of variation of these ratios in all Δt intervals is 0.339 to 0.505; overall distribution of values indicate a constancy of ratio from one Δt interval to another and no apparent difference between convergence and divergence. Therefore, the mean value of all ratios, 0.436, was used for computation and plotting of k(η) curves for convergence and divergence. Constancy of ratios from one Δt interval to another indicates constant decrease of convergent and divergent effects with increasing stability, because the convergence and divergence curves approach the normal curve as the stability index increases. Logical interpretation of this constant decrease indicates that stability resists all mixing forces equally.

Corresponding equations of convergence and divergence curves for a given Δt are:

$$\eta_{conv} = \left[\frac{1}{0.436} (k-k'_{conv}) 2p_{norm} \right]^{1/2} = \left[4.58 p_{norm} (k-k'_{conv})\right]^{1/2} \qquad (11)$$

$$\eta_{div} = \left[0.436 (k-k'_{div}) 2 p_{norm}\right]^{1/2} = \left[0.873 p_{norm} (k-k'_{div})\right]^{1/2} \qquad (12)$$

where $k'_{conv} = k'_{norm} - 0.07$ and $k'_{div} = k'_{norm} + 0.07$

Mixed-layer thickness is still correlated to wave parameters which must be taken from the wind field producing convergence or divergence at the point under consideration. This wind field usually lies outside the point of observation. This idea is based on the assumption that the area of observation or prediction was initially in the wind field where normal mixing occurred. Because of propagation of the wind field, the area later became a convergent or divergent zone, and the mixed-layer thickness was altered accordingly.

The upper and lower solid curves in Figures 15 through 22 for convergent and divergent conditions of pure wind current were computed by Equations (11) and (12). Only k and η values showing no intermixing of normal and convergent or divergent points (transition zones) were used

in computation of p values (Figure 23). Consequently, these curves must be considered to represent well-developed strong convergence or divergence effects on the mixed layer. In cases of weak or moderate convergent or divergent effects on the mixed layer, interpolations can be made between normal and convergent or divergent values. Successful interpolation depends considerably on experience and knowledge of local conditions.

$\bar{h}$ Curves

The broken-line curves in Figures 15 through 22 are used for determining the mixed-layer thickness $\bar{h}$ and were computed by Equation (7) after application of Equation (6) to determine k values for the various Δt intervals with known mixed-layer thickness and given wave parameters. After determination of the $k(\eta)$ curves, k values along with given wave parameters and the sea state parameter η were considered to be known. $\bar{h}$ values could then be computed and plotted as curves related to the $k(\eta)$ curves. The central $\bar{h}$ curve applies to normal mixing, the upper $\bar{h}$ curve applies to convergence, and the lower $\bar{h}$ curve applies to divergence. Mixed-layer thickness $\bar{h}$ is measured in feet and can be determined by means of the right half of the scale in the left margin of Figures 15 through 22. Intermediate values for weak or moderate convergent or divergent effects on the mixed layer may be interpolated between the normal and convergent or divergent values.

The $\bar{h}$ curves rise quite steeply for low η values, rise less steeply with moderate values, and finally level off at high η values. This leveling off occurs only with rather high η values at low stability indexes. With high values of stability index, leveling off begins for moderate values of η. The normal $\bar{h}$ curve for the Δt of 2° F is almost horizontal at an approximate η value of 620. This value of η corresponds to a fully developed sea in a wind field of 38 or 39 knots, where mixed-layer thickness is about 310 feet. Further increase of wind force would not appreciably increase the mixed-layer thickness, if normal conditions (no convergent effect) persist and Δt remains constant. In case of convergence the limit of $\bar{h}$ for the Δt of 2° F is about 450 feet at an η value of 885, which corresponds to about 43-knot winds and fully developed sea.

The normal $\bar{h}$ curve for the Δt interval of 17° F levels off when η equals 170, which corresponds to about 27-knot winds and fully developed sea. With such stability under normal mixing conditions (no convergent effect), further increase of wind force would not increase the mixed-layer thickness. Mixed-layer thickness at the Δt of 17° F is thus limited to 80 feet; the thickness could increase to about 135 feet, when η is 270 in the presence of a strongly developed convergent effect.

All $\bar{h}$ values and their limits apply only when $\overline{\Delta t}$ is constant. If the mixed-layer thickness increases rapidly, $\overline{\Delta t}$ does not usually remain constant. A mixture of cool water from the thermocline decreases the mixed-layer temperature and simultaneously decreases $\overline{\Delta t}$, so that the initial $\overline{\Delta t}$ value does not apply during the entire active mixing period. Lower $\overline{\Delta t}$ values must be substituted near the end of the mixing period; consequently, mixing

may be deeper than indicated by use of the initial stability index. If the surface temperature can be measured during the mixing period, a $\overline{\Delta t}$ value can be determined for use at the end of active mixing. The foregoing statements apply to all $\bar{h}$ curves.

Salinity Gradient

The surface and the 400-foot depths have been discussed as being the most convenient limiting levels for determination of the temperature difference between the surface and a level below the thermocline. A somewhat deeper level would be more convenient, because the thermocline sometimes extends below 400 feet. This temperature difference is used instead of the temperature gradient in the thermocline to represent stability; however, stability is a function of both temperature and salinity gradients. Internal waves and possibly other factors cause fluctuation of these gradients.

These fluctuations justify substitution of $\overline{\Delta t}$ for the mean temperature gradient in the thermocline without any great loss of accuracy, because $\overline{\Delta t}$ is considered proportional to the actual temperature gradient. When $\overline{\Delta t}$ remains nearly constant, the temperature gradient in the thermocline changes with decreasing thermocline and increasing mixed-layer thicknesses; however, change of the temperature gradient is incorporated in the function $k(\eta)$, and $\overline{\Delta t}$ efficiently substitutes for the actual temperature gradient in the thermocline.

Effect of the salinity gradient on stability has not been considered in calculations to this point. If the salinity gradient is positive, the maximum value is usually located somewhere in the deeper part of the thermocline, at a point below which salinity decreases slowly. The maximum value sometimes occurs below the thermocline. If the salinity gradient is negative its value usually decreases through the depth of the thermocline.

In order to simplify the stability factor, salinity differences in the thermocline are expressed as temperature differences and are designated $\Delta t'$. Thus $\Delta t'$ is an equivalent temperature difference that would produce a density change equal to that produced by a given salinity change in the thermocline. Temperature differences equivalent to salinity differences have been computed for a wide range of mean temperatures in the thermocline. Pressure and mean salinity effects in the thermocline are estimated to be negligible and have therefore been disregarded in this study. Increasing salinity with depth produces positive equivalent temperature changes ($\Delta t'^{+}$), and decreasing salinity with depth results in negative values ($\Delta t'^{-}$).

The result of 24 Nansen casts made in the thermocline at station CHARLIE in September 1960 is shown in Figure 26A. $\overline{\Delta t}'$ is 0.89° F. Data for salinity gradients in the thermocline during other months at this location were not available; however, an additional 43 observations from the same

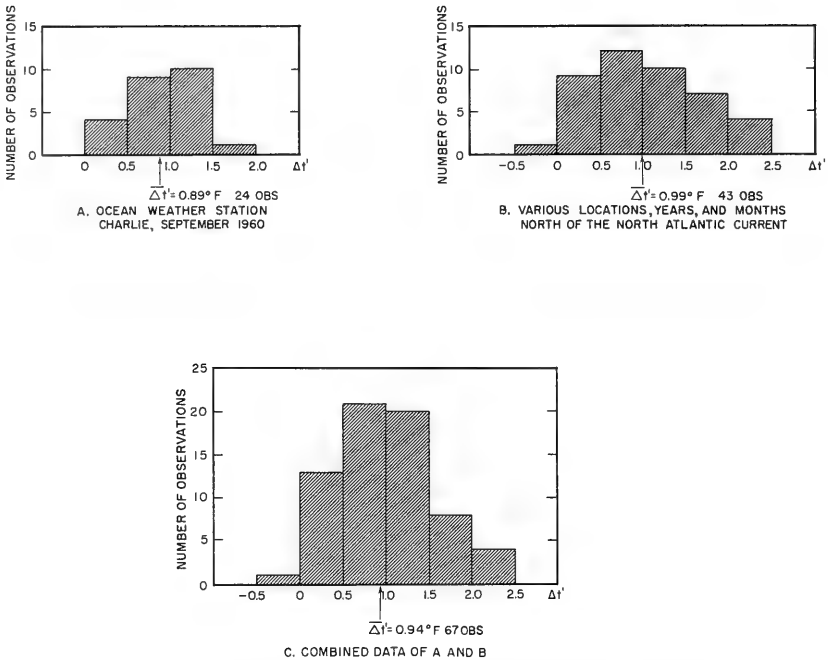

FIGURE 26 FREQUENCY DISTRIBUTIONS OF DENSITY CHANGES IN THE THERMOCLINE DUE TO SALINITY DIFFERENCES EXPRESSED AS TEMPERATURE DIFFERENCES $\Delta t'$ IN ° F

general area were available. The 43 observations are spread over several years and all months, excluding those of winter, and extend over a 10-degree square located immediately north of the North Atlantic Current. The result, shown in Figure 26B, is in good agreement with the data at station CHARLIE for September and more or less indicates the same salinity distribution throughout the months of the seasonal thermocline. These data are combined in Figure 26C.

The mean of the combined data ($\overline{\Delta t}' = 0.94^{\circ}$ F) must be the salinity effect on the $k(\eta)$ curves in Figures 15 through 22. It is assumed that this effect is incorporated in the stability indexes of these curves, so that the stability index of the $k(\eta)$ curves not only represents the mean temperature difference $\overline{\Delta T}$, but also $\overline{\Delta t}'$, the mean equivalent temperature difference which represents the mean salinity effect in the thermocline. Thus, $\overline{\Delta t}$ is the summation of $\overline{\Delta T}$ and $\overline{\Delta t}'$. The value of $\overline{\Delta t}'$ near station CHARLIE and in other temperate areas of the North Atlantic seems to be rather uniform and close to 1° F. If there is no salinity difference in the thermocline, 1° F should be subtracted from the temperature difference between the surface and 400 feet in order to obtain the correct value of $\overline{\Delta t}$.

The salinity gradient is apparently of little importance in areas north of the North Atlantic Current. The gradient becomes important to the south of this current, especially in major currents. Figure 27 shows the frequency distribution of $\Delta t'$ based on random observations in the area between the North Atlantic and the North Equatorial Currents. The range of $\Delta t'$ is -3° to $+3^{\circ}$ F; more than half of the salinity gradients were negative. In this area actual stability may be considerably different from that indicated by Δt, especially with negative salinity gradients. Since $k(\eta)$ curves correspond to 1° F higher stability indexes, the correction $C = -\Delta t' - 1^{\circ}$ must be applied in case of negative salinity gradients. For example, if $\overline{T}_o - \overline{T}_{400} = 10^{\circ}$ F, and the salinity difference in the thermocline corresponds to $\overline{\Delta t'} = -2^{\circ}$, the correction would be $C = -2^{\circ} - 1^{\circ} = -3^{\circ}$, and the actual stability index would be 7° F. This would correspond to stability produced by $\overline{T}_o - \overline{T}_{400} = 7^{\circ}$ F at constant salinity. If salinity increases with depth the correction is $C = \Delta t' - 1^{\circ}$; that is, no correction applies when $\Delta t' = 1^{\circ}$, a 1° correction applies when $\Delta t' = 2^{\circ}$ F, etc.

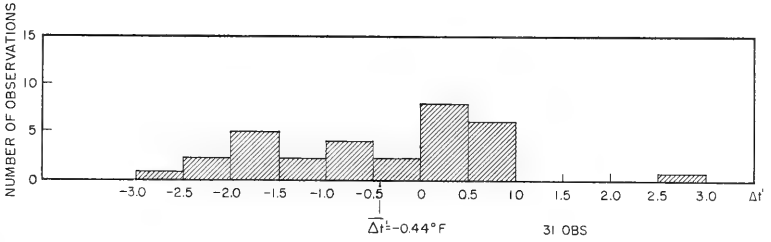

A. RANDOM OBSERVATIONS SOUTH OF THE NORTH ATLANTIC CURRENT

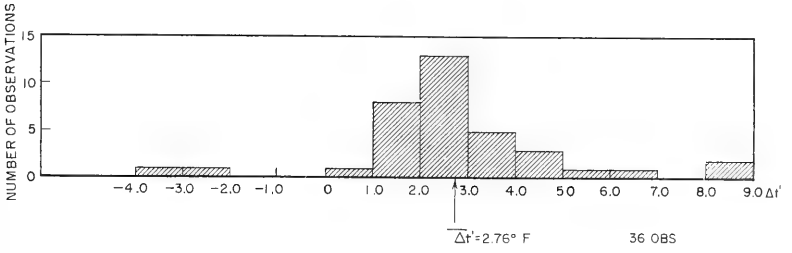

B. RANDOM OBSERVATIONS IN THE NORTH EQUATORIAL CURRENT, GULF STREAM, AND NORTH ATLANTIC CURRENT

FIGURE 27. FREQUENCY DISTRIBUTIONS OF DENSITY CHANGES IN THE THERMOCLINE DUE TO SALINITY DIFFERENCES EXPRESSED AS TEMPERATURE DIFFERENCES $\Delta t'$ IN °F

TABLE 4

CORRECTION OF STABILITY INDEXES FOR SALINITY DIFFERENCE IN THE THERMOCLINE

MEAN TEMPERATURE IN THE THERMOCLINE (°F)	CORRECTION* $\Delta t'$ (°F)									
	1	2	3	4	5	6	7	8	9	10
	SALINITY DIFFERENCE (°/oo) IN THE THERMOCLINE									
35	0.06	0.12	0.18	0.24	0.30	0.36	0.42	0.48	0.54	0.60
40	0.08	0.16	0.24	0.32	0.40	0.48	0.56	0.64	0.72	0.80
45	0.10	0.20	0.30	0.40	0.50	0.60	0.70	0.80	0.90	1.00
50	0.12	0.24	0.36	0.48	0.60	0.72	0.84	0.96	1.08	1.20
55	0.14	0.28	0.42	0.56	0.70	0.84	0.98	1.12	1.26	1.40
60	0.16	0.32	0.48	0.64	0.80	0.96	1.12	1.28	1.44	1.60
65	0.18	0.36	0.54	0.72	0.90	1.08	1.26	1.44	1.62	1.80
70	0.20	0.40	0.60	0.80	1.00	1.20	1.40	1.60	1.80	2.00
75	0.22	0.44	0.66	0.88	1.10	1.32	1.54	1.76	1.98	2.20
80	0.24	0.48	0.72	0.96	1.20	1.44	1.68	1.92	2.16	2.40
85	0.26	0.52	0.78	1.04	1.30	1.56	1.82	2.08	2.34	2.60

*If salinity increases with depth, the correction is positive and is reduced by 1° F. If salinity decreases with depth, the correction is negative and is increased by 1° F. No correction is applied if $\Delta t'$ equals 1° F.

Corrections are computed in Table 4 for various salinity differences for given mean temperatures in the thermocline. The above rules apply to the correction values taken from the table. For example, with mean temperature of 55° F and salinity difference of 0.42‰in the thermocline the general correction is 3°. If salinity decreases with depth 4° must be subtracted from $\overline{T}_o-\overline{T}_{400}$ to obtain the corrected value of $\overline{\Delta t}$; if salinity increases 2° must be added to $\overline{T}_o-\overline{T}_{400}$.

Figure 27 shows the frequency distribution of $\Delta t'$ in the North Equatorial Current, the Gulf Stream, and North Atlantic Current. Only 2 of the 36 observations showed negative salinity gradients. The remainder, which showed positive gradients,cover an extremely wide range of values. Analysis indicates that conclusions concerning stability in the currents based on temperature gradient alone have little meaning. For example, if $\overline{T}_o-\overline{T}_{400}$ = 10° F and $\Delta t'$ = 9° the actual stability index is 18° F, under constant salinity conditions. Therefore, the $k(\eta)$ curves in Figures 15 through 22 cannot be applied for prediction of thermocline thickness in currents,when salinity distribution in the thermocline is not known.

Excluding areas of permanent currents, salinity gradient corrections are required where salinity of surface water is increased by high evaporation during the time of the seasonal thermocline. In the Mediterranean Sea only 4 out of 25 observations showed a positive salinity gradient; the remainder showed negative gradients. Stability seems to be lower in the Mediterranean Sea for more time than the mean temperature difference (T_o-T_{400}) indicates. This is also probably true in all subtropical areas of the North Atlantic.

Weak Thermocline

Within the mixed layer a small thermocline, termed "weak thermocline," appears very often during decay of the mixed layer,when surface temperature rises and surface conditions supply only a small amount of mixing energy. There is probably no essential difference in formation of the weak thermocline,whether surface temperature increases are caused by advection or by other heating processes.

Temperature difference in the weak thermocline seldom exceeds 2° F; however, resulting stability is considerably stronger than normally expected. Figure 28 shows a plot of 21 k values determined for a weak thermocline by Equation (6). The normal (central) curve for the Δt interval of 11° F (Figure 19) has been fitted to the points to indicate how well their distribution agrees with the curve. In view of the small temperature difference in the weak thermocline, the point distribution would be expected to correspond more closely to the normal $k(\eta)$ curve for the Δt interval of 2° F (Figure 15). Such a high stability index, with consequent strong resistance to mixing by the weak thermocline, is difficult to explain. One possible explanation is that salinity increases considerably in the weak thermocline; however, the salinity increases could hardly account for the increase of equivalent stability index by as much as 8° F. The steep vertical temperat ure gradient in the weak thermocline may provide extra stability until a critical level of mixing energy prevails. This critical

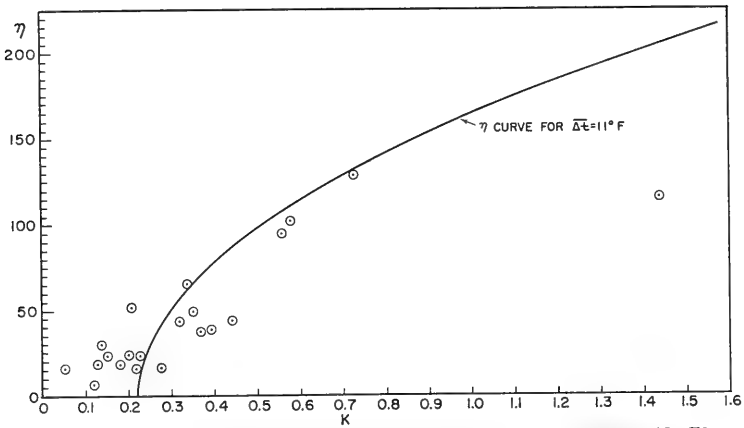

FIGURE 28 COMPARISON OF k(η) POINTS FOR A WEAK THERMOCLINE TO THE NORMAL k(η) CURVE FOR $\overline{\Delta t}$=11° F

level appears when the value of η reaches anywhere from 120 to 140, corresponding to a fully developed sea with 24- to 25-knot winds. Stronger surface conditions tend to destroy the weak thermocline and may eventually affect the main seasonal thermocline.

If the weak thermocline persists for several days, the lower part of the mixed layer often becomes part of the main thermocline, and eventually the weak thermocline becomes the interface between the mixed layer and the main thermocline as shown in Figure 29.

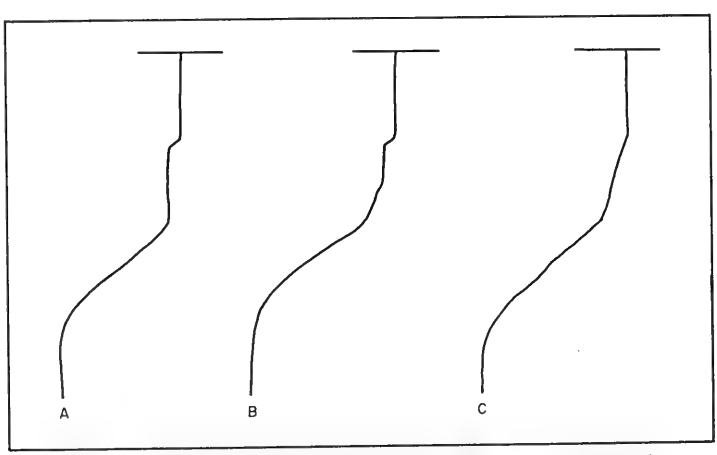

FIGURE 29 CONVERSION OF THE WEAK THERMOCLINE TO THE INTERFACE BETWEEN THE MIXED LAYER AND THE MAIN THERMOCLINE

The rather widely scattered distribution of points in Figure 28 does not permit definite conclusions. However, the normal curve for the Δt interval of 11° F (Figure 19) can be used to predict the weak thermocline depth, if there is evidence of surface temperature increase. Convergence and divergence effects probably enter the problem of predicting the weak thermocline depth and could partly account for the wide scattering of the points in Figure 28. Extent of decay in the lower part of the mixed layer depends largely on the strength of flow in the upper part of the thermocline.

Variation of Thermocline Depth With Latitude

Theoretical studies of thermocline depth have indicated a considerable increase of mixed-layer thickness with decreasing latitude, if wind conditions are the same. No empirical evidence to support such an increase can be found, and such conclusions are not substantiated by this study. Data from the North Atlantic at various locations between 35° and 56° N do not indicate measurable differences of mixed-layer thickness. Permanent convergence areas in subtropical zones may often be misleading; the rather thick mixed layer in such areas cannot be attributed to mechanical mixing. Strong negative salinity gradients in the thermocline often permit deeper mixing in these areas because of reduced stability. This fact may be one reason for the fictitious influence of latitude. If some small latitude effect is present, it may have been lost among several errors involved. For the time being, however, its existence and magnitude remain uncertain, and this prediction method can be considered valid for any latitude.

PRACTICAL PREDICTION OF THE THERMOCLINE DEPTH

Verification

The thermocline depth predicted by this method is the mean depth of the interface between the mixed layer and the thermocline. Consequently, verification of the prediction cannot be made with an individual BT observation, but must be determined from several (preferably 6 or more) BT observations taken over a period of about one day, because the amplitude of oscillation of the interface may be quite large. An individual BT is also a rather poor source for information concerning the temperature gradient in the thermocline and temperature distribution in the upper layers. Indeed, prediction of mean thermocline depth will often be more accurate and reliable than interpretation of the mean thermocline depth from a single BT observation.

Means of Prediction

Table 5 lists values of wave parameters and minimum fetch and duration for various wind speeds for fully developed sea. Only η values are required if the curves in Figures 15 through 22 are used. This η value is on the extreme left scale in the corresponding Δt graph. From the horizontal intersection of the η value with the proper $k(\eta)$ curve (normal,

TABLE 5

WIND AND SEA SCALE FOR FULLY DEVELOPED SEA

Beaufort Force	Wind Speed (knots)	Significant Height $H_{1/3}$ (feet)	Period of Maximum Energy of Spectrum T_{max}	Wave Length $\lambda = 3.41T^2_{max}$ (feet)	η	Minimum Fetch (nautical miles)	Minimum Duration (hours)
3	8.5	1.0	3.4	40	3.4	9.8	1.7
	10	1.4	4.0	55	6	10	2.4
	11	1.8	4.4	66	8	14	3.1
	12	2.2	4.8	79	11	18	3.8
4	13	2.7	5.2	92	14	23	4.5
	14	3.3	5.6	107	19	28	5.2
	15	4.1	6.1	125	23	34	5.9
	16	4.6	6.5	144	30	40	6.6
	17	5.4	6.9	162	37	48	7.5
5	18	6.1	7.2	176	44	55	8.3
	19	6.9	7.7	202	53	65	9.2
	20	8.0	8.1	224	65	75	10.0
	21	9.0	8.5	246	77	88	11.0
	22	10.0	8.9	270	89	100	12.0
	23	11.0	9.3	295	102	115	13.0
6	24	12.0	9.7	320	116	130	14.0
	25	13.7	10.2	355	140	155	15.5
	26	15.0	10.5	376	157	180	17.0
	27	16.0	10.9	405	180	205	18.5
	28	18.0	11.3	436	203	230	20.0
	29	20.0	11.7	467	236	255	21.5
7	30	22.0	12.1	499	266	280	23.0
	31	23.7	12.6	542	298	310	25.0
	32	26.0	12.9	567	336	340	27.0
	33	28.0	13.3	604	372	380	28.5
	34	30.0	13.6	631	408	420	30.0
	35	32.5	14.1	679	458	460	32.0
	36	35.0	14.5	718	508	500	34.0
8	37	37.0	14.9	758	551	530	37.0
	38	40.0	15.4	810	615	600	38.0
	39	42.5	15.8	850	671	655	40.0
	40	45.0	16.1	885	725	710	42.0
	41	47.5	16.6	940	788	770	44.5
	42	50.0	17.0	986	850	830	47.0
	43	54.0	17.4	1030	940	895	49.5
9	44	58.0	17.7	1070	1027	960	52.0
	45	61.0	18.2	1130	1110	1035	54.5
	46	64.0	18.6	1180	1190	1110	57.0

convergent, or divergent), proceed vertically to the intersection with the corresponding dashed curve, h(k). Horizontally from this intersection, the thermocline depth ($\overline{h}$) is determined on the second scale at the left of the graph.

For application of this prediction method in non fully developed sea, $H_{1/3}$ and T_{max} are taken from graphs for non fully developed sea in H.O. Pub. 603, and η is computed in the usual way ($\eta = HT$).

Determination of the Stability Index

The stability index, Δt, must be determined and corrected for the salinity gradient, if possible, before a prediction can be made. Improved accuracy of Δt can be obtained by averaging temperature differences between the surface and the 400-foot level from 4 to 6 BT's covering a 24-hour period. Such opportunities seldom exist. In fact, predictions would be less difficult if frequent BT's were made. Usually, the best situation will include BT's taken up to several days earlier in a nearby area.

The most likely sources of such observations are "Selected BT Charts" of the North Atlantic which are transmitted daily by facsimile from the Hydrographic Office. These charts are compiled from BT messages from various ships and may contain as many as 22 observations distributed throughout the North Atlantic. Observation points other than weather ship locations may change from day to day. Reference to recent BT charts may provide satisfactory observations for the area under consideration.

$\overline{\Delta t}$ computed from several BT's, even though they might have been taken a few days apart, is preferable because of the short range oscillations of temperature at 400 feet due to internal waves. In the absence of advection, surface temperatures do not change significantly in periods of less than 5 to 10 days. Mean temperature variation at 400 feet would be even less; however, instantaneous temperature measurements may vary considerably from the mean. When observations are not available for the immediate area, the stability index can be evaluated by interpolation from 2 or more BT's proximal to the prediction area, provided that neither was taken in an area of permanent currents.

Statistical computations of temperatures at the surface and at 400 feet and of Δt for limited areas, perhaps 5 degrees square, would be of some help. However, data for such complete coverage are not available. Figures 30, 31, and 32 represent monthly frequency distributions of Δt at stations CHARLIE, DELTA, and ECHO. Table 6 contains ranges, means, and standard deviations of temperatures and Δt at the surface and 400 feet for these stations.

Station DELTA is located in the North Atlantic Current; therefore, statistical results for this station are quite different from those for stations CHARLIE and ECHO. The mean of all standard deviations for DELTA is 34 percent larger than the mean of all standard deviations for CHARLIE and 37 percent larger than the mean of all standard deviations for ECHO.

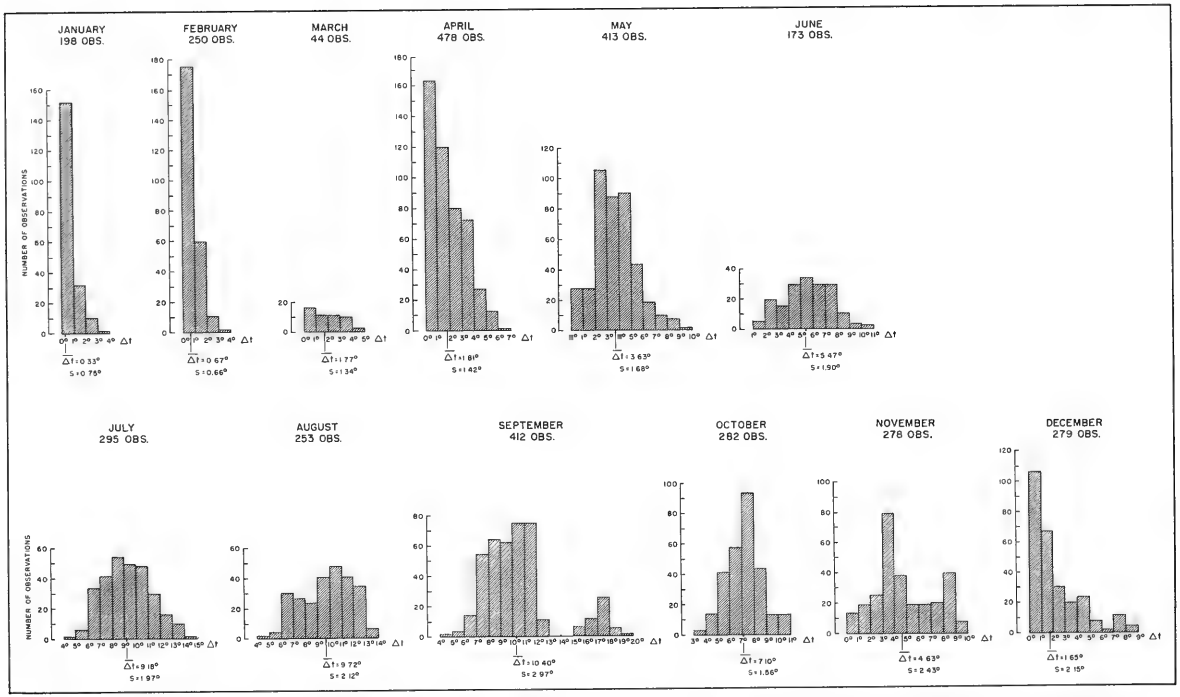

FIGURE 30 MONTHLY FREQUENCY DISTRIBUTION OF STABILITY INDEX Δt (° F) AT OWS CHARLIE (52° 48' N, 35° 30' W, 13 YEARS' DATA)
$\overline{\Delta t}$ = MEAN MONTHLY STABILITY INDEX, S = STANDARD DEVIATION

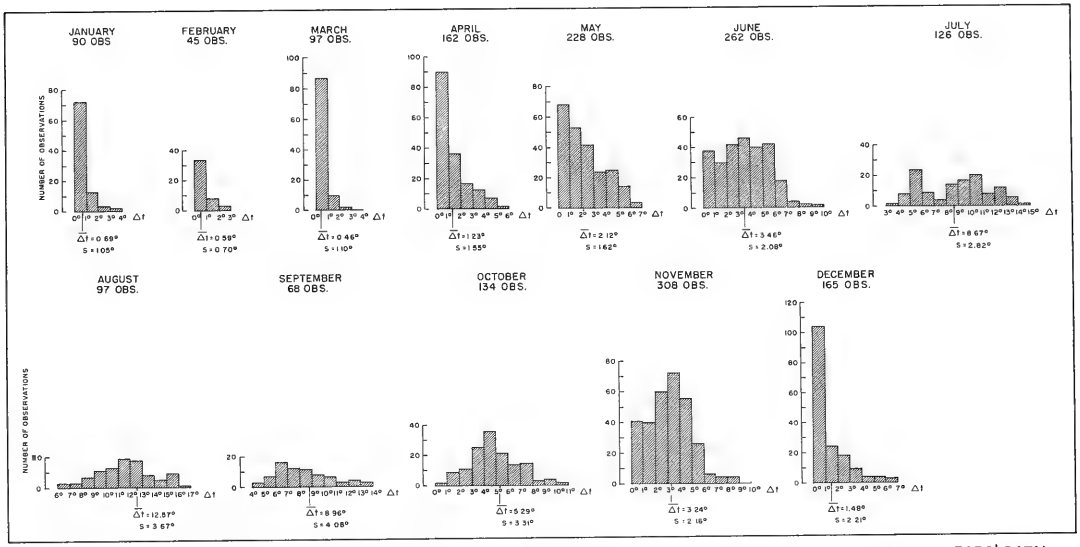

FIGURE 31 MONTHLY FREQUENCY DISTRIBUTION OF STABILITY INDEX Δt (° F) AT OWS DELTA (44° N, 41° W, 13 YEARS' DATA)
$\overline{\Delta t}$ = MEAN MONTHLY STABILITY INDEX, S = STANDARD DEVIATION

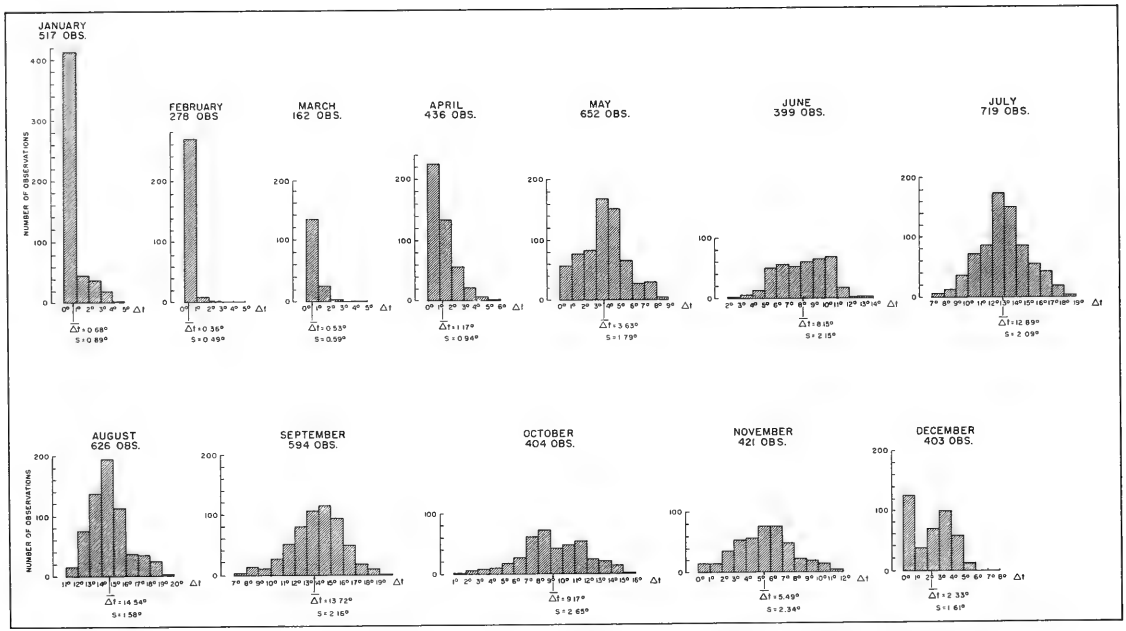

FIGURE 32 MONTHLY FREQUENCY DISTRIBUTION OF STABILITY INDEX Δt (° F) AT OWS ECHO (35° N, 48° W, 16 YEARS' DATA)
$\overline{\Delta t}$ = MEAN MONTHLY STABILITY INDEX, S = STANDARD DEVIATION

TABLE 6

MEAN MONTHLY TEMPERATURE AND Δt VALUES, THEIR RANGES AND STANDARD DEVIATIONS AT THREE OCEAN WEATHER STATIONS

		CHARLIE (52° N, 35° W; 13 years' data)				DELTA (44° N, 41° W; 13 years' data)				ECHO (35° N, 48° W; 16 years' data)			
		Temp. and Δt range (°F)	Mean of Temp. and Δt (°F)	S.D.	Obs.	Temp. and Δt range (°F)	Mean of Temp. and Δt (°F)	S.D.	Obs.	Temp. and Δt range (°F)	Mean of Temp. and Δt (°F)	S.D.	Obs.
Jan.	Surface	38-49	43.48	2.17	416	52-69	59.74	4.02	179	64-73	67.01	1.87	659
	400 feet	38-48	43.36	1.92	289	52-68	59.40	4.00	155	62-73	66.35	1.72	568
	Δt	0-4	0.33	0.75	198	0-4	0.69	1.05	90	0-5	0.68	0.89	517
Feb.	Surface	38-48	43.25	1.87	386	51-66	59.37	3.55	91	60-73	66.62	2.16	546
	400 feet	38-47	42.83	1.76	306	51-64	58.44	3.03	66	60-72	66.47	2.09	376
	Δt	0-4	0.67	0.66	250	0-3	0.59	0.70	45	0-3	0.36	0.49	278
Mar.	Surface	39-48	44.14	1.63	185	51-66	58.50	3.30	209	59-71	65.09	1.63	327
	400 feet	39-46	42.33	1.57	51	51-64	57.99	2.18	141	59-70	64.70	1.87	211
	Δt	0-5	1.77	1.34	44	0-3	0.46	1.10	97	0-3	0.53	0.59	162
Apr.	Surface	40-51	45.20	1.88	607	52-68	58.63	3.54	282	59-73	64.85	2.37	654
	400 feet	40-49	43.67	1.97	499	52-67	58.12	2.98	236	60-69	64.06	1.47	452
	Δt	0-7	1.81	1.42	478	0-6	1.23	1.55	162	0-6	1.17	0.94	436
May	Surface	40-54	46.01	2.26	559	51-66	59.02	3.44	278	59-74	67.56	2.10	882
	400 feet	40-49	42.51	1.56	414	51-63	57.10	3.26	258	59-69	63.82	1.62	655
	Δt	0-10	3.63	1.68	413	0-7	2.12	1.62	228	0-9	3.63	1.79	652
June	Surface	43-55	48.64	2.60	272	57-70	63.63	3.32	324	65-77	72.26	2.60	572
	400 feet	40-48	43.51	1.75	173	54-65	60.18	1.91	275	60-68	64.08	2.10	401
	Δt	1-11	5.47	1.90	173	0-10	3.46	2.08	262	2-14	8.15	2.15	399
July	Surface	46-56	51.93	2.29	530	65-77	70.38	2.89	162	71-85	77.63	1.83	867
	400 feet	40-50	43.18	1.68	295	56-67	62.10	2.39	127	60-70	64.72	1.77	726
	Δt	4-15	9.18	1.97	295	3-16	8.67	2.82	126	7-19	12.89	2.09	719
Aug.	Surface	49-58	52.91	1.84	471	68-81	72.50	2.82	122	72-82	79.38	1.52	757
	400 feet	40-50	43.12	1.50	254	52-67	60.01	4.27	113	60-70	64.83	1.51	626
	Δt	4-14	9.72	2.12	253	6-17	12.57	3.67	97	11-20	14.54	1.58	626
Sep.	Surface	49-61	53.56	2.42	566	64-74	67.31	3.68	113	71-84	79.13	1.52	763
	400 feet	39-48	43.30	1.84	413	50-66	58.71	5.60	76	60-72	65.48	2.00	595
	Δt	4-20	10.40	2.97	412	4-14	8.96	4.08	68	7-19	13.72	2.16	594
Oct.	Surface	46-54	50.17	1.65	412	61-73	66.41	3.54	166	70-81	75.09	2.02	558
	400 feet	39-48	43.22	1.79	286	54-69	61.35	4.56	140	60-74	65.03	2.80	404
	Δt	3-11	7.10	1.56	282	0-11	5.29	3.31	134	1-16	9.17	2.65	404
Nov.	Surface	42-52	48.13	1.93	371	57-72	65.87	3.53	453	68-78	72.76	1.65	529
	400 feet	39-48	43.58	1.84	279	53-71	63.75	3.55	391	61-75	67.22	2.82	422
	Δt	0-10	4.63	2.43	278	0-10	3.24	2.16	308	0-12	5.49	2.34	421
Dec.	Surface	37-52	45.00	2.33	470	55-69	62.80	2.63	337	66-78	70.53	2.25	553
	400 feet	37-49	43.39	3.14	339	53-68	62.38	2.92	273	63-76	68.14	3.13	423
	Δt	0-9	1.65	2.15	279	0-7	1.48	2.21	165	0-6	2.33	1.61	403

Mean values of Δt at all stations follow an annual wave pattern rather consistently. Except for temperatures at the 400-foot level at station DELTA, the mean monthly temperatures also generally fit the annual wave pattern. Mass advection apparently plays an important part in temperature distribution of area DELTA. It should be noted that the number of observations for this station is considerably less than those available for other areas.

During winter months, the frequency distribution of Δt is strongly skewed, and the range of Δt is quite limited. Such a distribution is understandable because the mixed-layer thickness is generally greater than 400 feet during these months. When heating of surface water increases, the frequency distribution becomes more symmetrical and often approaches the normal distribution. Double maxima patterns, similar to those occurring in September and November in Figure 30 or in July in Figure 31, are due to anomalous data of one or a few years for these months. The anomalies may be caused by erroneous BT's or by mass advection which may persist for several weeks. Some BT data are questionable, owing to prolonged use of unreliable instruments.

Temperature values at the 400-foot level generally follow the trend of values at the surface during the seasonal thermocline. If the surface temperature is a few degrees higher than the mean during a given month, the mean temperature at 400 feet can also be expected to be higher than the mean at the 400-foot level. The mean temperature at the 400-foot level during any month is rather stable; therefore, the range of Δt should be small. The range appears rather large, however, during the seasonal thermocline, because instantaneous temperatures taken at 400 feet often show large oscillations due to internal waves at the bottom of the thermocline.

Δt values that lie approximately within the limits of standard deviations in frequency distributions can be termed "real"; values near the flanks, however, should be called "apparent", because the majority of them are produced by short-term temperature oscillations at the 400-foot level.

Statistical values are computed from the collective data for a 5-degree square around the center of each of the 3 stations. The combined areas of these squares represent only a small fraction of the North Atlantic; therefore, mean values of temperatures and stability indexes can serve only as general information and for comparison with other information.

Prediction of Mixed-Layer Decay and Associated Thermocline Depth

Conditions are uncertain after active mixing ceases and decay of the mixed layer begins. This situation may be partially relieved by surface conditions which might exert a mixing force on the mixed layer. The question is: How deep will the force penetrate? If it penetrates to the bottom of the mixed layer, decay will be prevented; if it does not extend to the bottom of the mixed layer, decay may advance upward to the level of effective mixing. In either case mixing always takes place in the mixed layer

under neutral stability conditions; however, a certain amount of mixing must occur at the interface to prevent formation of a density gradient in the lowest portion of the mixed layer. The stability index of 2° F used in this prediction method is the nearest interval to neutral stability conditions ($\Delta t = 0^{\circ}$). The mixing force necessary to insure decay resistance at the region of interface may occur at this low Δt interval.

In order to clarify this idea, suppose a 30-knot wind and a fully developed sea exist in the prediction area. Stability index at the time of prediction is 7° F; furthermore, the sea state parameter η, determined from Table 5, is 266. The predicted mean thermocline depth from the normal curve in Figure 17 is 165 feet. If there is a 25-knot wind and a fully developed sea on the following day, significant wave height ($H_{1/3}$) will be at least 13.7 feet, T_{max} will be 12.2 seconds, and η will equal 140. The mixing force is smaller than it was on the previous day; consequently, the thickness of the mixed layer will not be increased unless convergence is produced by the 30-knot wind field. Figure 15 ($\Delta t = 2^{\circ}$ F) shows that mixing could effectively penetrate the mixed layer to 200 feet at this η value. Sufficient mixing takes place in the lowest part of the mixed layer to prevent decay (formation of density gradient), and the thermocline depth will remain 165 feet, as long as the latter surface conditions persist. Suppose the wind is 20 knots 2 days later. The sea state parameter η for fully developed sea is then 65, and the effective mixing penetrates to only 135 feet (Figure 15). This means that the mixed-layer thickness should decrease from 165 feet to 135 feet, if the same surface conditions persist for several days.

Mixed-layer decay has been predicted quite successfully during tests of this method; however, data are insufficient to recommend its use as standard procedure. The method may be correct, but numerous other factors may be involved. Decay depends not only on residual mixing but also on flow in the thermocline, on convergence or divergence, and on other factors which are not usually known.

Persistence

This prediction method does not require knowledge of previous temperature distribution and mixed-layer thickness. If a prediction is made every day over a long period of time in the same area and proper verifications can be made with BT observations, "persistence" (of the previously observed thermocline depth) can be taken into account. Predictions can then be adjusted, especially if there is a tendency towards convergence or divergence which is not clearly apparent from weather charts. Persistence is valid as long as the same surface conditions exist. Since changes of thermocline depth usually occur slowly, the persistence method of forecasting is successful a large percentage of the time. However, if mixing energy overcomes stability at the interface or if favorable conditions occur for decay of the mixed layer, persistence disappears. A prediction can then be based only on the changing factors.

Although a prediction method based on mixing and stability factors is always preferable, persistence should be consulted for adjustment of the prediction if there is sufficient reason to believe that such an adjustment is necessary or useful.

The method of prediction developed in this study can generally be used anywhere in the ocean without previous information on the mixed layer and thermocline; the only requirement is knowledge of the surface wind waves and the stability index.

If prediction of the thermocline depth is desired for an area where no observations or predictions have been made or where none have been made for the past 10 or more days, weather conditions in the area for at least the past 20 days must be studied. If low or moderate wind sea has prevailed for the last 10 days and a heavy storm has occurred within the past 12 to 15 days, it is reasonable to determine: (1) At what depth was the thermocline established during the storm? and (2) Was the thermocline depth increased by convergence after the storm? Answers to these questions provide the initial value of mixed-layer thickness from which loss of thickness due to decay must be subtracted to determine present mixed-layer thickness.

If no great perturbations occurred during the previous few weeks and if surface conditions remained approximately the same for a longer period of time, the prediction can be based on the average existing surface conditions.

Examples of Prediction

Example 1 - The wind field at the prediction point (52°48' N, 35°30' W) is shown in Figure 33. Mean wind was about 24 knots from the northeast

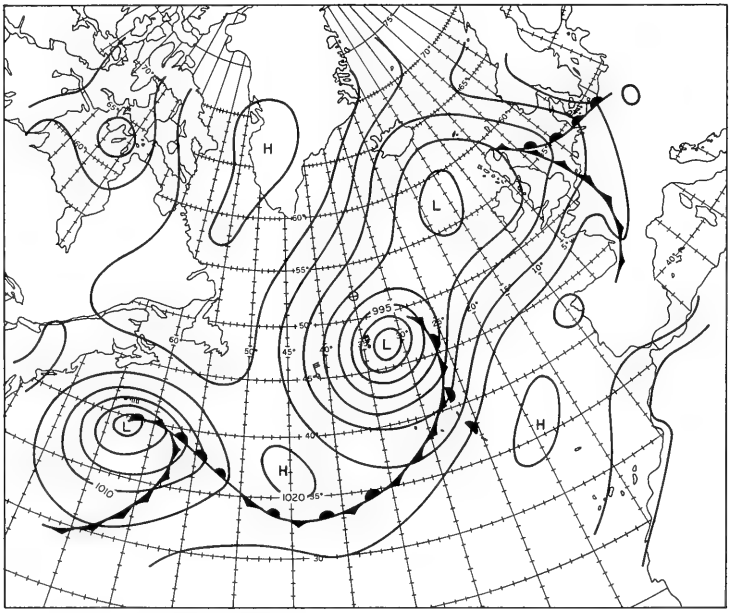

FIGURE 33 NORMAL WIND FIELD AT A PREDICTION POINT (52° 48' N, 35° 30' W) — 1230Z, 12 JUNE 1951

over a period of 35 hours, and fetch was about 400 to 500 nautical miles; therefore, the sea was fully developed. Stronger winds did not occur for approximately 3 previous weeks. From Table 5 the sea state parameter η equals 116. Stability index was about 9° F. Convergence or divergence effects are not evident; therefore, the case is considered to be normal. From the central solid and dashed (normal) curves in Figure 18, the predicted thermocline depth $\overline{h}_p$ is 127 feet.

Three BT observations were made on the prediction day. Thermocline depth was 133 feet at 1000Z, 131 feet at 1400Z, and 110 feet at 1800Z. The mean observed thermocline depth $\overline{h}_o$ was 125 feet.

Example 2 - The prediction point (52°48' N, 35°30' W) shown in Figure 34 has been situated at the western edge of a storm for about 8 days. On 27 and 28 March, wind force at the point and eastward from it was about 40 to 45 knots; during the next 6 days, wind force was about 30 to 35 knots in the wind field east of the prediction point. Mean wind was about 35 knots in the entire wind field over the 8-day period, and minimum fetch condition was satisfied; therefore, the sea was considered fully developed.

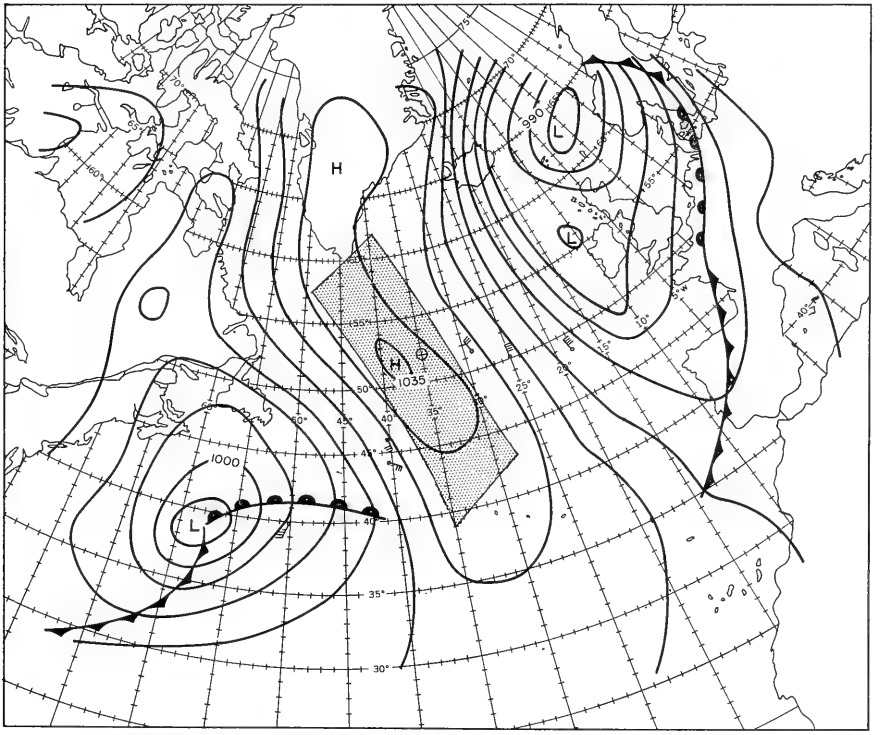

FIGURE 34 CONVERGENCE EFFECT CAUSED AT A PREDICTION POINT (52° 48' N, 35° 30' W) BY A WIND FIELD TO THE EAST. 1230Z, 3 APRIL 1953 — SHADED AREA INDICATES THE APPROXIMATE CONVERGENCE ZONE.

Since wind direction and position of the wind field with respect to the prediction point did not change for about 8 days, a well-developed convergence effect could be expected at the prediction point. The value of η for wind speed of 35 knots and fully developed sea is 458 (Table 5). Stability index was about 2° F. By application of the upper solid and dashed (convergence) curves in Figure 15, the predicted mean thermocline depth $\overline{h}_p$ is 388 feet.

The mean observed thermocline depth computed from 8 BT's taken during 3 days (2-5 April) was 370 feet.

Example 3 - The prediction point ($52^{\circ}48'$ N, $35^{\circ}30'$ W) lay in a divergence zone within cyclonic wind fields for about 40 hours. The center of this cyclone moved into the prediction area during the afternoon of 29 May and remained stationary until 1230Z 31 May as shown in Figure 35.

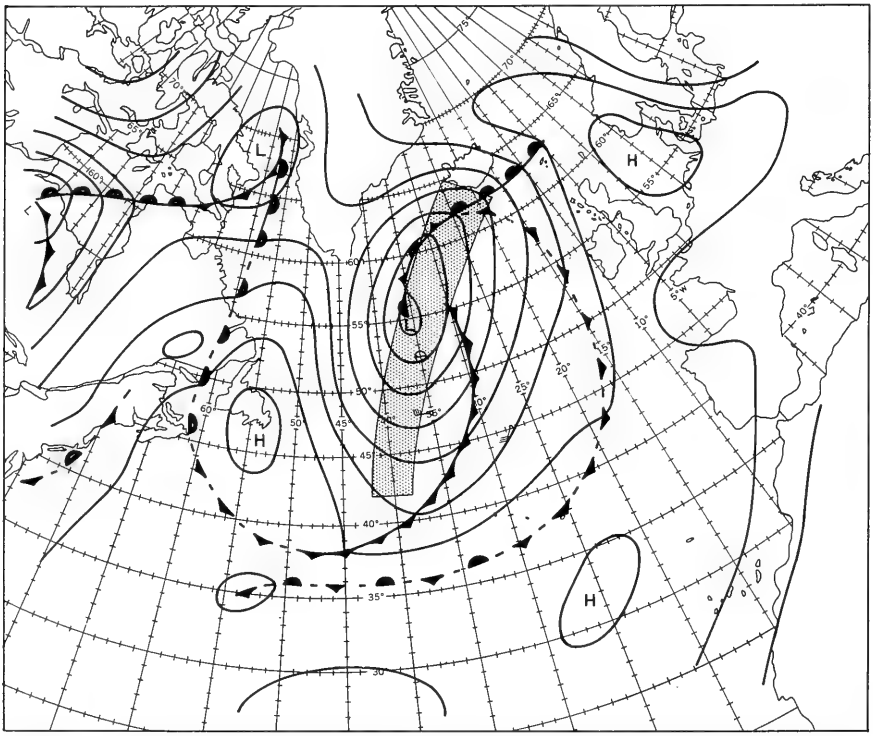

FIGURE 35 DIVERGENCE EFFECT CAUSED AT A PREDICTION POINT (52° 48' N, 35° 30' W) BY WIND FIELDS TO THE NORTHWEST AND SOUTHEAST. 1230Z, 31 MAY 1950 — SHADED AREA INDICATES THE APPROXIMATE DIVERGENCE ZONE.

The mean wind at both sides of the divergence zone was evaluated to be 28 knots for 30 hours. Both fetch and duration were sufficient for fully developed sea. The sea state parameter η from Table 5 is 203. Stability index was between 6° and 7° F. From the lower solid and dashed (divergence) curves in Figure 17, predicted thermocline depth at this η value is 109 feet.

The mean observed thermocline depth computed from 3 BT's taken between 0900Z and 1600Z on 31 May was 100 feet.

Approximation

The variables and conditions considered in this prediction method seem to be acting logically in the right directions and proportions. The method is far from being exact, but the degree of approximation can be improved.

The first source of inexactness may lie in the prediction technique. The mixing factor k and the $k(\eta)$ curves were developed empirically from rather limited data. Determination of 356 values of k distributed over 8 intervals of stability indexes does not provide good concentration of points; therefore, the curves in Figures 15 through 22 may shift somewhat from their actual positions. Such deviation should produce a systematic error, the extent of which cannot be evaluated at present; however, this error is assumed to be rather small when compared with other causes of error.

Inexactness produced by incorrect evaluation of parameters will cause a random error which may often be quite large, especially if several components of this error should possess the same algebraic sign. The first of these erroneous components is introduced by inexact evaluation of the wind field and, consequently, erroneous wave parameters. This error is largest for weak winds and low stability indexes and is least with strong winds and high stability indexes.

Error Due to Wind Evaluation and Decrease of Error With Increasing Wind

With a stability index of 9°, 15-knot winds in a normal field, and fully developed sea, predicted thermocline depth would be 86 feet. Under these same conditions with 16-knot winds, the depth would be 108 feet. Thus, erroneous evaluation of mean wind speed by one knot in this example would produce a difference of 22 feet in the prediction. With the same stability index, 26-knot winds, and fully developed sea, predicted thermocline depth would be 139 feet; whereas, with 27-knot winds it would be 142 feet - now the difference is only 3 feet.

Error Due to Wind Evaluation and Decrease of Error With Increasing Δt

With a stability index of 2°, 23-knot winds in a normal field, and fully developed sea, predicted thermocline depth would be 167 feet. Under these same conditions with 24-knot winds, the depth would be 182 feet.

The difference is 15 feet. With a stability index of 13°, the same winds would give predicted thermocline depths of 102 and 108 feet, respectively - now the difference is only 6 feet.

Error Due to Stability Index Evaluation

The second component of random error is introduced by erroneous evaluation of the stability index. This error is more likely to occur than that of erroneous wind evaluation, because of (1) the uncertainties and lack of direct means for evaluating Δt, and (2) the error due to correction for a salinity gradient.

With a stability index of 5°, 25-knot winds in a normal field, and fully developed sea, predicted thermocline depth would be 165 feet. The predicted depth with a stability index of 7° would be 148 feet. The difference is 17 feet.

Error Due to Type of Current Field

Another component of random error is inexact evaluation of the type of current produced by the wind field, whether it is normal (horizontal flow), convergent, or divergent. This error is largest for low stability indexes and decreases somewhat as stability index increases.

If a fully developed sea with 25-knot winds is erroneously interpreted as being strongly convergent while it is actually normal, the error in predicted thermocline depth would amount to 52 feet for the Δt interval of 2° and 40 feet for the Δt interval of 13°.

Evaluation of the rate of convergence or divergence is a difficult task. Furthermore, methods for determining the existence of convergence or divergence are mainly subjective. For the time being, it is quite satisfactory to determine one of the three types of rate of convergence or divergence (weak, moderate, and strong) with a good approximation. The solid upper and lower curves in Figures 15 through 22 correspond to strong convergence and divergence. Moderate and weak rates must be interpolated between the normal (central) and the corresponding upper or lower curve. Convergence or divergence produced by pure wind current depends considerably on local and seasonal conditions; for example, permanent horizontal flow, vertical boundaries, mean vorticity, permanency of the convergence or divergence, prevailing angle between direction of wind and propagation of the wind field, barometric pressure, upwelling, etc. This error should gradually decrease as experience in a given area increases.

Components of random error are also produced by factors other than those considered in this prediction technique. Most important of these are mixing processes which may be acting concurrently with mechanical processes to increase or decrease the total mixing effect. Of these, instability mixing due to evaporation and surface cooling can be very significant, especially in late fall.

Table 7 shows the results of a test consisting of 216 predictions and hindcasts at stations BRAVO, CHARLIE, and DELTA. A prediction was made for each day on which at least 3 BT's were available for verification. Predictions were scattered randomly over several years for all months of the seasonal thermocline. Corrections of stability index for salinity were not possible because salinity gradients were not known. BRAVO and DELTA are located in permanent currents, where salinity gradients and their variations may often be very large. Prediction conditions at these locations can be considered very unfavorable, while prediction conditions at CHARLIE are rather favorable.

Although Table 7 gives a general view of the test, it is somewhat distorted, because the prediction error in feet for shallow thermoclines is a large percentage of the observed depth; whereas the same error in feet for deep thermoclines is a small percentage of the observed depth.

The data used for compiling Table 7 were also used to compute the mean values of the observed thermocline depth and of the prediction error for each station of the test (Table 8).

As mentioned previously, ECHO (35° N, 48° W) seems to lie in an area of permanent convergence during late summer and autumn. This area is not convergent during spring and early summer. A test of 21 predictions was made at this station in April, May, June, and July. The results of this test are included in Table 8. Distribution of negative and positive errors of prediction at BRAVO, CHARLIE, DELTA, and ECHO does not indicate variability of thermocline depth with latitude.

Figure 36A shows the frequency distribution of absolute values of prediction errors in percent of the mean observed thermocline depth. This figure was constructed from the combined data of Table 7 and hindcasts for ECHO during spring and early summer. Figure 36B shows the frequency distribution of the same data at CHARLIE and ECHO only. Nine hindcasts with widely scattered errors exceeding 50 percent of the observed thermocline depth were excluded from the frequency distribution in Figure 36A, although they are included in Table 7. No such prediction errors occurred at CHARLIE and ECHO. The 9 omitted cases were made in areas of permanent currents and were all positive. Some of these errors were apparently caused by failure to recognize convergent or divergent effects during prediction. The error was less than 10 percent of the observed thermocline depth 50 percent of the time in Figure 36A and was less than 10 percent of the observed value 65 percent of the time in Figure 36B.

Figure 36C shows the frequency distribution of negative and positive errors from the observed values of the same data in Figure 36A. The mean of the errors $\bar{\epsilon}$ is -1.8 percent. The negative shift is mainly caused by excessive negative errors at CHARLIE. Since data of CHARLIE were used to develop this prediction method, a closer balance between negative and positive errors than would occur at the other stations can be expected. Examination of weather data for hindcasts revealed a general tendency to underestimate the rate of convergence when hindcasting thermocline depth. Frequent convergence in the area of CHARLIE is quite strong, because water

TABLE 7

FREQUENCY (PERCENT) OF PREDICTION ERRORS OF THERMOCLINE DEPTH AT STATIONS BRAVO (56°30' N, 51°W), CHARLIE (52°48' N, 35°30' W), and DELTA (44°N, 41°W)

BRAVO			CHARLIE			DELTA		
Difference between predicted and observed thermocline depth (percent of observed)	Number of predictions and hindcasts	Percent of total	Difference between predicted and observed thermocline depth (percent of observed)	Number of predictions and hindcasts	Percent of total	Difference between predicted and observed thermocline depth (percent of observed)	Number of predictions and hindcasts	Percent of total
<5	14	20	<5	35	42	<5	10	15
<10	24	35	<10	54	69	<10	24	35
<15	35	51	<15	67	86	<15	35	51
<20	46	67	<20	73	94	<20	43	62
<30	56	81	>20	5	6	<30	55	80
>30	13	19				>30	14	20
Total	69			78			69	

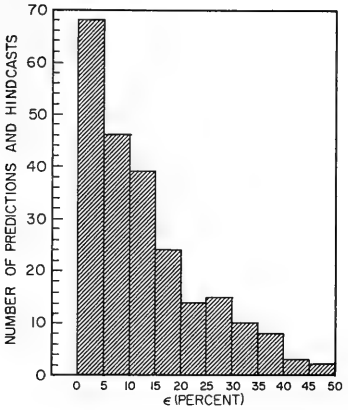

A. ABSOLUTE VALUES OF ERRORS AT ALL STATIONS

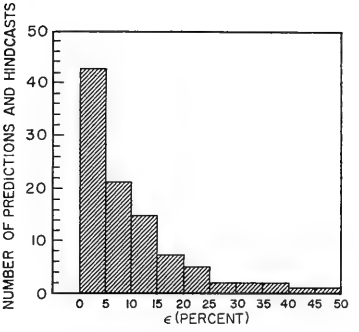

B. ABSOLUTE VALUES OF ERRORS AT CHARLIE AND ECHO

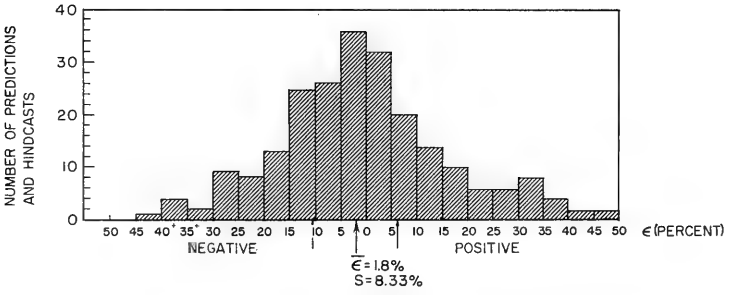

C. POSITIVE AND NEGATIVE VALUES OF ERRORS AT ALL STATIONS

FIGURE 36 FREQUENCY DISTRIBUTION OF ERRORS BETWEEN PREDICTED OR HINDCAST DEPTH AND OBSERVED THERMOCLINE DEPTH AT STATIONS BRAVO, CHARLIE, DELTA, AND ECHO

TABLE 8

MEAN VALUES OF PREDICTION ERRORS

Station	Mean observed thermocline depth (ft) $\bar{h}_o$	Mean neg. value of prediction error (ft) $\bar{\epsilon}^-$	Mean abs. value of prediction error (ft) $\overline{\lvert\epsilon\rvert}$	Mean pos. value of prediction error (ft) $\bar{\epsilon}^+$	Mean error from observed (percent)	No. of neg. errors	No. of pos. errors
BRAVO*	141.9	21.6	23.9	25.9	16.8	33	36
CHARLIE*	162.8	14.2	12.7	11.3	7.8	46	32
DELTA*	136.5	21.6	23.6	25.7	17.3	37	32
ECHO**	102.5	9.4	12.8	14.9	12.5	9	12

* All months of seasonal thermocline
** April, May, June, and July only

transport of pure wind current in the area is usually forced against permanent flow on the western side of a cyclonic wind field.

The standard deviation of errors S is 8.33 percent. About one-half of the hindcasts falls within the standard deviation limits.

CONCLUSIONS

This method of thermocline depth prediction is mainly limited with respect to time by limitations of weather prediction. With some experience in ocean regions where permanent currents are not present, the predictor can be expected to forecast with an error of less than 10 percent of the observed depth about 70 percent of the time. More exact and regular data are required for improvement of prediction. Present approximations allow the following conclusions:

The mixed layer during the seasonal thermocline is primarily produced by mechanical mixing due to wind waves and pure wind currents.

With the same rate of mixing energy, the mixed-layer thickness is inversely proportional to stability in the thermocline.

Convergence produced by pure wind current increases mixed-layer thickness in areas where no convergence formerly existed. Likewise, divergence produced by pure wind current decreases the mixed-layer thickness in areas where no divergence formerly existed.

Decay of the mixed layer depends on the depth to which existing mechanical mixing energy can penetrate under nearly neutral stability conditions.

The predicted thermocline depth is the mean level of the interface between the mixed layer and the thermocline.

Predicted distribution of instantaneous depths of the interface in any area will be possible only after sufficient knowledge concerning the spectral distribution of internal waves has been gained.

Knowledge of the effects of instability mixing acting concurrently with mechanical mixing could improve prediction of the thermocline depth during time of the seasonal thermocline.

The distribution of the mixed layer and thermocline is a complex problem. Because of this complexity, many different approaches are possible. Other thermocline prediction methods with the same or better approximation will probably be devised. The combination of several methods may lead to dependable prediction of the thermocline depth several days or weeks in advance for all oceans.

ACKNOWLEDGEMENT

Help and suggestions rendered by various personnel of the Oceanographic Prediction Division and by the officers and crew of the USCGC CHINCOTEAGUE, whose kind collaboration during September 1960 enabled collection of valuable supplemental data, are gratefully acknowledged.

BIBLIOGRAPHY

DEFANT, ALBERT. Turbulenz und Vermischung im Meer. Deutsche Hydrographische Zeitschrift, Band 7, Heft 1/2. 13 p. 1954.

FREEMAN, JOHN C., JR. Note on a prediction equation for the surface layer of a two layer ocean. A & M College of Texas, Dept. of Oceanography, Technical Report No. 5. 5 p. 1953.

KITAIGORODSKII, S. A. On the computation of the thickness of the wind mixing layer in the ocean. Izvestiia Academy of Sciences, USSR Geophysics Series No. 3. p. 425-431, March 1960.

LAEVASTU, T. Factors affecting the temperature of the surface layer of the sea. Havsforskningsinstitutets Skrift No. 195 Helsinki. 136 p. 1960.

MUNK, W. H. and ANDERSON, E. R. Notes on a theory of the thermocline, Journal Marine Research. vol. 7, no. 3. 20 p. 1948.

PIERSON, W. J., NEUMANN, G., and JAMES, R. W. Practical methods for observing and forecasting ocean waves by means of wave spectra and statistics, U. S. Hydrographic Office Publication No. 603. 284 p. 1955.

SCHULE, J. J., JR. Effects of weather upon the thermal structure of the ocean. U. S. Navy Hydrographic Office Publication Misc. 15360. 81 p. 1952.

ROSSBY, C. G. and MONTGOMERY, R. B. The layer of frictional influence in wind and ocean currents. MIT and WHOI, vol. III, no. 3. 101 p. 1935.

NOMENCLATURE

A	Wave amplitude $\frac{H_{1/3}}{2}$
G	Vertical density gradient
G_t	Vertical temperature gradient
h	Mixed-layer thickness or thermocline depth
$H_{1/3}$	Significant wave height
k	Mixing parameter
p	Parameter of the conic (distance from vertex to focus)
T_{max}	Period of maximum energy of the wave spectrum
Δt	Stability index
$\Delta t'$	Stability correction for salinity
ϵ	Error of prediction
η	Sea state parameter ($H_{1/3}T_{max}$)
λ	Wave length
ρ	Density

U. S. Navy Hydrographic Office.
PREDICTION OF THE THERMOCLINE DEPTH by P. A. Mazeika, June 1960. 80 p. including 36 figs. (H. O. TR-104, ASWEPS REPORT No. 5).

Bibliography

A method of predicting the thermocline depth has been devised using BT data and weather conditions at ocean weather station CHARLIE (52°N, 35°W). Mean BT data were used to determine a mixing parameter associated with sea state. Stability in the thermocline and extent of convergence or divergence in wind-driven currents are used to predict the thermocline depth at any point.

1. Thermocline
2. Thermal Structure
3. Oceanography
4. ASWEPS

i. title: Prediction of the thermocline depth

ii. author: P. A. Mazeika

iii. H. O. TR-104

U. S. Navy Hydrographic Office.
PREDICTION OF THE THERMOCLINE DEPTH by P. A. Mazeika, June 1960. 80 p. including 36 figs. (H. O. TR-104, ASWEPS REPORT No. 5).

Bibliography

A method of predicting the thermocline depth has been devised using BT data and weather conditions at ocean weather station CHARLIE (52°N, 35°W). Mean BT data were used to determine a mixing parameter associated with sea state. Stability in the thermocline and extent of convergence or divergence in wind-driven currents are used to predict the thermocline depth at any point.

1. Thermocline
2. Thermal Structure
3. Oceanography
4. ASWEPS

i. title: Prediction of the thermocline depth

ii. author: P. A. Mazeika

iii. H. O. TR-104

U. S. Navy Hydrographic Office.
PREDICTION OF THE THERMOCLINE DEPTH by P. A. Mazeika, June 1960. 80 p. including 36 figs. (H. O. TR-104, ASWEPS REPORT No. 5).

Bibliography

A method of predicting the thermocline depth has been devised using BT data and weather conditions at ocean weather station CHARLIE (52°N, 35°W). Mean BT data were used to determine a mixing parameter associated with sea state. Stability in the thermocline and extent of convergence or divergence in wind-driven currents are used to predict the thermocline depth at any point.

1. Thermocline
2. Thermal Structure
3. Oceanography
4. ASWEPS

i. title: Prediction of the thermocline depth

ii. author: P. A. Mazeika

iii. H. O. TR-104

U. S. Navy Hydrographic Office.
PREDICTION OF THE THERMOCLINE DEPTH by P. A. Mazeika, June 1960. 80 p. including 36 figs. (H. O. TR-104, ASWEPS REPORT No. 5).

Bibliography

A method of predicting the thermocline depth has been devised using BT data and weather conditions at ocean weather station CHARLIE (52°N, 35°W). Mean BT data were used to determine a mixing parameter associated with sea state. Stability in the thermocline and extent of convergence or divergence in wind-driven currents are used to predict the thermocline depth at any point.

1. Thermocline
2. Thermal Structure
3. Oceanography
4. ASWEPS

i. title: Prediction of the thermocline

ii. author: P. A. M

iii. H. O. TR-104

U. S. Navy Hydrographic Office.
PREDICTION OF THE THERMOCLINE DEPTH by P. A. Mazeika, June 1960. 80 p. including 36 figs. (H. O. TR-104, ASWEPS REPORT No. 5).

Bibliography

A method of predicting the thermocline depth has been devised using BT data and weather conditions at ocean weather station CHARLIE (52°N, 35°W). Mean BT data were used to determine a mixing parameter associated with sea state. Stability in the thermocline and extent of convergence or divergence in wind-driven currents are used to predict the thermocline depth at any point.

1. Thermocline
2. Thermal Structure
3. Oceanography
4. ASWEPS

i. title: Prediction of the thermocline depth
ii. author: P. A. Mazeika
iii. H. O. TR-104

U. S. Navy Hydrographic Office.
PREDICTION OF THE THERMOCLINE DEPTH by P. A. Mazeika, June 1960. 80 p. including 36 figs. (H. O. TR-104, ASWEPS REPORT No. 5).

Bibliography

A method of predicting the thermocline depth has been devised using BT data and weather conditions at ocean weather station CHARLIE (52°N, 35°W). Mean BT data were used to determine a mixing parameter associated with sea state. Stability in the thermocline and extent of convergence or divergence in wind-driven currents are used to predict the thermocline depth at any point.

1. Thermocline
2. Thermal Structure
3. Oceanography
4. ASWEPS

i. title: Prediction of the thermocline depth
ii. author: P. A. Mazeika
iii. H. O. TR-104

U. S. Navy Hydrographic Office.
PREDICTION OF THE THERMOCLINE DEPTH by P. A. Mazeika, June 1960. 80 p. including 36 figs. (H. O. TR-104, ASWEPS REPORT No. 5).

Bibliography

A method of predicting the thermocline depth has been devised using BT data and weather conditions at ocean weather station CHARLIE (52°N, 35°W). Mean BT data were used to determine a mixing parameter associated with sea state. Stability in the thermocline and extent of convergence or divergence in wind-driven currents are used to predict the thermocline depth at any point.

1. Thermocline
2. Thermal Structure
3. Oceanography
4. ASWEPS

i. title: Prediction of the thermocline depth
ii. author: P. A. Mazeika
iii. H. O. TR-104

U. S. Navy Hydrographic Office.
PREDICTION OF THE THERMOCLINE DEPTH by P. A. Mazeika, June 1960. 80 p. including 36 figs. (H. O. TR-104, ASWEPS REPORT No. 5).

Bibliography

A method of predicting the thermocline depth has been devised using BT data and weather conditions at ocean weather station CHARLIE (52°N, 35°W). Mean BT data were used to determine a mixing parameter associated with sea state. Stability in the thermocline and extent of convergence or divergence in wind-driven currents are used to predict the thermocline depth at any point.

1. Thermocline
2. Thermal Structure
3. Oceanography
4. ASWEPS

i. title: Prediction of the thermocline depth
ii. author: P. A. Mazeika
iii. H. O. TR-104

Given in Loving Memory of

Raymond Braislin Montgomery
Scientist, R/V Atlantis maiden voyage
2 July - 26 August, 1931
****
Woods Hole Oceanographic Institution
Physical Oceanographer
1940-1949
Non-Resident Staff
1950-1960
Visiting Committee
1962-1963
Corporation Member
1970-1980
******
Faculty, New York University
1940-1944
Faculty, Brown University
1949-1954
Faculty, Johns Hopkins University
1954-1961
Professor of Oceanography,
Johns Hopkins University
1961-1975